EVALUATION OF A MICROFLOWMETER AND DEVELOPMENT OF A MICROFLUIDIC VALVE

By

KARTHIK PITCHAIMANI

A THESIS PRESENTED TO THE GRADUATE SCHOOL
OF THE UNIVERSITY OF FLORIDA IN PARTIAL FULFILLMENT
OF THE REQUIREMENTS FOR THE DEGREE OF
MASTER OF SCIENCE

UNIVERSITY OF FLORIDA

2008

To my grandparents

ACKNOWLEDGMENTS

I would like to acknowledge Dr. Fan for guiding me through my curriculum. His training in research and presentation skills has been of immense value to me. I would like to thank Dr. Nishida for his regular feedback and evaluation which helped me toward the right direction. I thank Dr. Schmitz for serving on my supervisory committee.

I would like to thank Brian Sapp for heater fabrication, Adam Winter and Joey Wilson for making the printed circuit board, and Daniel Olivero and Austin Gispanski for help in fabricating devices and topas film device picture. For general thought-provoking, brainstorming sessions and discussions I acknowledge Dr. Champak Das, Ruba Khnouf, Zheng Xia and Dr. Hong Chen. I gratefully acknowledge the support and cooperation from all past and present group members in Dr.Fan's Lab.

Finally, I acknowledge the greatest support I received from my family. They motivated me toward my goal to strive and achieve excellence.

TABLE OF CONTENTS

page

ACKNOWLEDGMENTS 4

LIST OF TABLES 7

LIST OF FIGURES 8

ABSTRACT 9

CHAPTER

1 INTRODUCTION 11

1.1 Microfluidics 11
1.2 Microvalves 12
1.3 Study Overview 14

2 EVALUATION OF A MICROFLOWMETER AND ITS USE IN TESTING A MICROVALVE 16

2.1 Introduction 16
2.2 Experimental Section 17
2.2.1 Device Fabrication 17
2.2.2 Flow Rate Measurement 18
2.3 Results and Discussion 19
2.3.1 Flow Meter Calibration 19
2.3.2 Flow Measurement in Devices 20
2.3.3 Flow Pulsations 21
2.3.4 Microvalve Testing Using Flowmeter 23
2.4 Conclusion 25

3 FABRICATION AND CHARACTERIZATION OF A THERMALLY ACTUATED MICROFLUIDIC VALVE 34

3.1 Introduction 34
3.2 Brief Review of Microvalves 34
3.3 Principle of Operation 36
3.4 Experimental Section 36
3.4.1 Device Fabrication for Microvalve 36
3.4.2 Elastomeric Film 37
3.4.3 Polyester (PET) Film 37
3.4.4 Microheaters 39
3.4.5 Thermal Fluid 40

3.4.6 Valve Characterization 41
3.4.6.1 Electric-current method 41
3.4.6.2 Temperature measurement 42
3.4.6.3 Fluorescence measurement 43
3.5 Results and Discussion 43
3.5.1 Device Fabrication 43
3.5.1.1 Heater fabrication and integration 44
3.5.1.2 Fluorinert encapsulation 44
3.5.2 Valve Characterization 45
3.5.2.1 Cyclic valve operation 45
3.5.2.2 Actuation time 46
3.5.2.3 Operating temperature 46
3.5.2.4 Valve operation with liquid pressure: pumping and hydrostatic head 48
3.5.2.5 Fluorescence measurement 50
3.6 Conclusion 51

4 CONCLUSIONS AND FUTURE WORK 67

4.1 Microvalve Fabrication 67
4.2 Microvalve Operation 67
4.2.1 Evaluation Using a Flow Meter 67
4.2.2 Electric Current Measurement 68
4.3 Future Work 69

LIST OF REFERENCES 70

BIOGRAPHICAL SKETCH 75

LIST OF TABLES

Table page

1-1 Comparison of different micromachined valve actuation mechanisms.....15

2-1 The volume of syringes and parameters of syringe pump 27

3-1 Elastomer film properties.....53

3-2 Hydrostatic heads and flow rates.....53

LIST OF FIGURES

Figure		page
2-1	Experimental setup.	28
2-2	Comparison of the flow rates measured by the direct method and the Sensirion flowmeter	28
2-3	Comparison of the flow rates measured by the Sensirion flowmeter in the presence and absence of a microfluidic device.	29
2-4	Comparison of the flow rates measured by the Sensirion flowmeter in two setups using stiff or flexible tubing..	30
2-5	Temporal profiles of flow rates measured by the Sensirion flowmeter in different setups..	31
2-6	Microfluidic valve..	32
2-7	Microvalve actuation data recorded by flowmeter showing the local flow dynamics.	33
3-1	Microfluidic valve concept based on thermal actuation principle..	54
3-2	Multilayer microvalve device.	54
3-3	Electric-current method to study valve actuation..	55
3-4	Labview GUI for data acquisition during valve testing.	56
3-5	Valve actuation when 58 mW was applied to Au heaters.	58
3-6	Valve actuation time as a function of the input power..	59
3-7	Temperature at different locations during valve actuation at 58 mW input heater power.	60
3-8	Temperature at different locations of a microvalve as a function of power.	62
3-9	Valve actuation for a 300 nL/min flow with different heater input powers..	63
3-10	Electric current as a function of time when different hydrostatic heads were used..	64
3-11	Fluorescent images showing valve action.	65
3-12	PCB connected to a microvalve device.	66

Abstract of Thesis Presented to the Graduate School
of the University of Florida in Partial Fulfillment of the
Requirements for the Degree of Doctor of Philosophy

EVALUATION OF A MICROFLOWMETER AND DEVELOPMENT OF A MICROFLUIDIC VALVE

By

Karthik Pitchaimani

December 2008

Chair: Hugh Fan
Cochair: Toshikazu Nishida
Major: Mechanical Engineering

Microelectronics was the technological revolution of the 20th century highlighting the power of miniaturization. Extension of the same into chemistry and life sciences is projected to be one of the next most significant scientific developments. Microfluidics implements this principle by reducing the size of a lab to that of a chip, aptly called “Lab on a chip” (LOC). This downsizing has several predicted advantages including lower reagent consumption, faster analysis, higher separation resolution and detection sensitivity, and lower detection limit. For nearly the past 20 years many researchers have developed conceptual LOC devices to address various applications including DNA amplification in a chip.

Several constituent elements are required to make a LOC system. Valves are one of the critical components which help control fluid flows in a microdevice. They are used for fluid containment, isolation and directing flows. Conventional MEMS (Micro-electro-mechanical system) based valves are made mostly on silicon whose integration with LOC tend to be problematic. Primary problems include optical clarity, difference in operational conditions, and suitability to gas rather than liquids.

As a solution, a thermally actuated microfluidic valve is developed in this work for plastic microfluidic devices. The principle of operation is based on a thermally sensitive fluid, which expands to actuate a membrane that controls the fluid flow. The power input for thermal expansion is controlled using a printed circuit board (PCB) which is suited to mass production and large scale integration. The microfluidic valve was fabricated and its operation has been demonstrated. Its operating parameters including actuation times, range of operational power and repetitive operation have been studied. The temperature during operation was also measured.

Two methods were used to test the valve operation. First method involves a flowmeter which was used to measure flow downstream. The flowmeter was evaluated for general microfluidic applications for this purpose. In the evaluation, the flowmeter was calibrated using direct method where the amount of water collected over a known period was weighed. It was also used to study the effect of stiffness of the tubing connecting the pump to the microfluidic device. Stiff tubing was found to maintain accurate flow rate. Existence of pulsations in flow was confirmed due to the use of syringe pump. Pulsations were dependent on tubing stiffness, presence of microfluidic device, flow rate and syringe size.

The second method was based on measurement of the electric-current in a channel and it was used to study the local valve action. Fluorescence was also used to qualitatively show valve action. The valve was found to operate over a wide range of power from 36 mW to 80 mW with valve close and open response times in seconds. The local channel temperature during valve operation was found to be less that 45 degree centigrade. The valve can operate as many as 50 times when the hydrostatic head was 9.5 mm. The valve was reliable when the flow rate was as high as 300 nL/min (1.2 mm/s).

CHAPTER 1
INTRODUCTION

Technology has always played a critical role in changing the way of our lives. Invention of the wheel is an example of the earliest development to have made a considerable impact on the society. In the recent times, one such revolutionary technology is the science of microelectronics and microfabrication. Starting from the thought provoking speech by Richard Feynman[1] and the invention of Integrated circuits[2] this technology has come a long way in influencing our day-to-day activities. In the latter part of the 20th century microfabrication was adopted towards modeling of miniature physical systems (transducers) in the form of Micro-electro-mechanical systems (MEMS).[3, 4] The extension of MEMS and application of microfabrication to chemistry and life sciences was realized later on. Notably the seminal paper by Manz[5] brought the new application field into notice. The concept of miniaturizing laboratory instruments has heralded a new stream of research with considerable promise. This science was termed as the miniaturized total analyses system (μTAS) where the concept of lab on a chip was initiated.[5, 6]

1.1 Microfluidics

Microfluidics is the science of manipulating fluids in micron scale.[6] It is the technology behind realizing a μTAS where fluid flows in microchannels are needed. The predicted advantages of miniaturization propel increasing number of researchers to work in this field.[7] Some advantages are apparent such as point of care applications, clinical diagnostics, remote monitoring and analysis due to its portability. Other advantages are owing to scaling which include reduction in reagent volume, shorter reaction times for biological and chemical applications resulting in smaller time constants, higher detection sensitivity, lower detection limits and lower costs with mass production.[5-7]

Several publications demonstrate the feasibility of this principle[8-11] in an attempt to fabricate a complete lab-on-a-chip (LOC) incorporating sample introduction, pretreatment, analysis (reaction or separation) and finally detection. In addition, the high throughput predicted for LOC application have also been demonstrated in the form of large scale integrated microfluidic platforms.[12] Present progress in attaining a reliable μTAS are reviewed in some reports[13-15] highlighting the achievements and further improvements needed to realize the potential promised by the technology.

Initially, silicon was the primary substrate material used in the microfabricated analysis systems owing to the existing, developed silicon fabrication technologies. However lack of optical transparency and the issues involved in fabrication made researchers pursue glass and recently polymers[16, 17] such as polydimethylsiloxane (PDMS),[18-23] polycarbonate,[24] polymethymethacrylate,[25, 26] and cyclo olefin copolymer[27] as the alternative materials. Plastics offer the most lucrative properties in terms of ease of fabrication, lower cost for mass production and optical clarity.

There are several components that are required to make a successful LOC platform. Valves, pumps, mixers are some of the most important ones to name. These components are the building blocks of a LOC device needed to manipulate fluid samples. One of the main reasons why μTAS has not been widely commercially implemented is the lack of reliable components, which has proved to be a primary hindrance in realizing the potential of LOC systems.[28] This thesis will focus on the development of a novel microfluidic valve to address the needs of present LOC systems.

1.2 Microvalves

Several attempts have been made to fabricate reliable microfluidic valves; however, there is still room for improvement in terms of performance. Conventional MEMS-based microvalves

have been developed as early as the solenoid valve fabricated by Terry et al.[3] for his gas chromatographic air analyzer. The valve was based on a solenoid plunger actuating a nickel diaphragm that controls the flow in conjunction with the valve seat. In general, majority of the valves were fabricated in silicon substrate using the micromachining technology. Their target applications were primarily MEMS based device integration. However, with the introduction of μTAS these principles were adapted to microfluidic platforms and several newer materials were also being increasingly used as a substrate for microvalve.

Microvalves are primarily classified into active and passive, depending upon the operational mechanism. Active microvalves need external stimulus in the form of electromagnetic,[3] electrostatic,[29] piezoelectric,[30, 31] pneumatic,[19, 32] thermopneumatic,[33-39] and shape memory alloy[40] (SMA) etc. In addition, there are several phase change microvalves making use of hydrogel,[41, 42] paraffin,[43, 44] polyethylene glycol.[45] Passive microvalves make use of inherent characteristics of the system and are based on surface effects such as capillarity.[46, 47] Each of these has its own advantages and limitations. A thorough review of the microvalves can be found in the recent publication by Ahn et al.[28]. The traditional text by Shoji[48] and Kovacs[49] also summarizes these data. Table 1-1 compares the characteristics of these principles. The fastest actuation times are achievable through electrostatic microvalves. However their low stroke and pressure coupled with very high voltage requirements limit their application. Piezoelectric actuators are fast with large force but produce very small strokes. The need of high voltage also restricts its use. Although pneumatic microvalves produce large stroke and pressure they are slow in response. Additionally, they need bulky accessories that affect device portability. One of the most widely used valve actuation mechanism is thermal. At the small scale, this method has been attractive, due to low thermal mass.[49] It generates large pressure and

deflection with moderately fast actuation times. However, it needs proper temperature control so that it will not affect the sample being analyzed.

1.3 Study Overview

In order to achieve the true potential of a lab-on-a-chip in terms of high throughput a microvalve needs to be fabricated which is compatible with large scale integration. Adaptability to industrial fabrication is another critical factor. Keeping these applications in mind along with the various ideal characteristics of a microvalve[49] a solution has been proposed and demonstrated in this thesis. A thermally actuated microfluidic valve has been developed and it can be controlled with a printed circuit board (PCB). Supplying heat to thermally sensitive fluid results in its expansion. This increase in volume has been used to deflect an elastomeric film into the microfluidic channel. Thermal expansion of the fluid was at a temperature well below the boiling point thus there is no phase change. This avoids excessive heating of samples. The thermally sensitive fluid was heated using a resistive heater fabricated using standard lithographic patterning procedures. The power supply to the heater can be controlled using a PCB, making it adaptable to industrial applications. A thermally actuated valve has been fabricated and the concept is demonstrated in this work.

Table 1-1. Comparison of different micromachined valve actuation mechanisms[28, 48]

	Electromagnetic	Piezoelectric	Pneumatic	Electrostatic	Thermopneumatic
Stroke	Large	Small	Large	Small	Large
Response time	Fast	Fast	Slow	Very fast	Medium
Pressure or Force	Small	Large	Large	Small	Large
Remarks	Fabrication complexity	Large voltage	Bulky accessories	Extremely high voltage	Heat input

CHAPTER 2
EVALUATION OF A MICROFLOWMETER AND ITS USE IN TESTING A MICROVALVE

2.1 Introduction

Flow control and metering of liquids in nanoliters are often required in microfluidic devices. For devices using electroosmotic pumping, flow rates can be calculated from the applied electric field and osmotic mobility.[8] For devices employing pneumatic pumps, flow rates can be estimated by the pumping rate.[50] However, these methods do not enable us to detect flow variations in microchannel, for example, due to the change in the surface charges in an electro-osmotic flow or spatial restrictions in a pressure-driven flow. Other possibilities that lead to flow rate changes include head loss[51] due to the dead volume and geometry mismatch in macro-to-micro interfaces,[52] flow variation due to the stretching of flexible tubing that connects pumps with devices, flow resistance caused by packed columns,[50] and blockage resulting from microfluidic valves.[19, 53]

For some applications, it is not critical to know exact flow rates; an approximate value from calculation or estimation suffices. However, knowing accurate flow rates is a necessity for other applications. For instance, the mixing ratio of a sample and a buffer solution must be precisely measured and controlled so that the actual sample concentration analyzed in the device is accurate for quantification.[9] An unaccounted change in the flow rate could lead to inaccurate reporting and documentation of the sample. Also when a microfluidic valve is present in a fluid network, flowmeters are required to monitor local flow rates to detect if the flow is truly blocked without leakage.[19, 53]

The physical principles that can be used in flowmeters have been reviewed by Nguyen.[54] Many efforts described in this review are based on silicon-based traditional MEMS (Micro-electro-mechanical systems) and developed primarily for gases. A few recent efforts have

focused on microscale liquid flow measurement, including thermal flow sensors,[53, 55] electrochemical velocimetry,[56] electronic current monitoring,[57, 58] particle image velocimetry (PIV),[59, 60] and laser induced fluorescence photo-bleaching anemometer.[61] However, all of them either have difficulty in measuring instantaneous velocity or require specialized hardware that is not readily commercially available.[61]

One commercially available flowmeter that was developed for microfluidic applications is SLG 1430 from Sensirion AG (Zurich, Switzerland).[62, 63] Two models (SLG 1430-025 and SLG 1430-150) are compatible with most microfluidic devices. The operational flow rate for SLG 1430-025 ranges from 50 nL/min to 1500 nL/min while that for SLG 1430-150 is 250 nL/min to 7000 nL/min according to the manufacturer. The flowmeter is based on thermal sensing and the sensors are fabricated using standard integrated circuit fabrication techniques.[62, 63] Since the flowmeter has not been extensively exploited in microfluidic research, SLG 1430-150 flowmeter was evaluated in this study and employed to measure and analyze the flow rate variations due to the presence of a microfluidic valve in a flow circuit. In the evaluation process, the effect of the stiffness of tubing used to connect a syringe pump with a microfluidic device on the flow rate in the device was studied. Also, the flowmeter was used to confirm the existence of flow pulsation resulting from a syringe pump as suspected.[64, 65] It was found that the degree of flow pulsation was reduced when flexible tubing was used and/or when a microfluidic device was connected in the fluid network. It was also dependent on the size of syringe used in the pump.

2.2 Experimental Section

2.2.1 Device Fabrication

Plastic microfluidic devices were fabricated using the procedure described previously.[27] Briefly, a photomask pattern was designed using AutoCAD and then reproduced in glass using photolithography. By electroplating on the glass plate, a nickel alloy mold was generated and

then used to produce plastic parts from cyclo-olefin resins (Zeonor 1020R) using a Carver hydraulic press (Wabash, IN). A CNC milling machine was employed to trim the plastic parts into 1 x 3 in. substrates and drill 2-mm-diameter holes at the channel ends. The substrate was then sealed with a 250-µm-thick film (Zeonor 1020R) from PLITEK (Des Plaines, IN) using a Catena thermal laminator (Northbrook, IL). The holes at channel ends became wells for fluid connections. A picture of the device is shown in Figure 2-1. The device is 1.5 mm thick while all channels in the microfluidic device are 74 µm wide and 27 µm deep. The cross section of the channels is D-shaped due to isotropic etching of the glass substrate that was used for fabricating the molding master.[27] The length of the channel used in this work is 26 mm.

2.2.2 Flow Rate Measurement

The experimental setup in Figure 2-1 was used for flow rate measurement. A UMP-II syringe pump from World Precision Instruments, Inc. (Sarasota, FL.) was controlled by a Micro4 controller. It was used with a 100-µl gastight Hamilton 1710LT syringe (Reno, Nevada) for the reagent delivery in all experiments except for one, in which a 250-µL liquid-tight SGE syringe was used. The pump controller was set to syringe type "G" and "H" for the 100-µl and 250-µl syringes, respectively, according to the manufacturer's instructions. The syringe was connected to one well (the inlet) of the microfluidic device using a tube (#1) and Upchurch Nanoport fittings (Oak Harbour, WA). The outlet of the channel was connected via another tube (#2) to a Sensirion SLG1430-150 flowmeter (Zurich, Switzerland). The fluid out of the flowmeter was collected through a tube into a microcentrifuge tube.

Two types of tubes with different stiffness were used for tube 1. One was an Upchurch PEEK tube with 100 µm ID and 1.57 mm OD that will be referred to as a "stiff" tube in the text. The other is a Corning silicone tube with 300 µm ID and 0.64 mm OD referred to as a "flexible" tube in the text. The stiff tube was expected to maintain the pumping pressure generated from

the syringe pump while the flexible tube diminished the pumping pressure to a certain degree. Tube 2 is an Upchurch PEEK capillary tube with 100 μm ID and 360 μm OD. A stiff tube was always used for tube 2 so that the flow rate measured by the flowmeter truly reflects the value in the device.

Purified water was used as the reagent except where specified otherwise. It was purified by a Barnstead Nanopure water system (Dubuque, Iowa). The flow rate was set by the syringe pump, ranging from 250 nL/min to 7000 nL/min, which corresponds to 2.5 to 70 mm/s calculated using the cross section area of the channels in the device. It was then measured by the Sensirion flowmeter and the data was acquired by a computer and graphical user interface (GUI) provided by the flowmeter manufacturer. The data readout frequency can be selected from 1.56 Hz to 200 Hz. A high frequency (200 Hz) was used to collect the initial data for displaying fast changing flows while a low frequency (3.12 Hz) was employed to study microvalve actuation. The flow rate was further calibrated using a direct method,[51] which was to measure the amount of water that accumulated in a container over a fixed time period. The collected water was weighed by a Fisher accu-124 analytical balance (Pittsburgh, PA) with an accuracy of 0.1 mg. The volumetric flow rate was calculated by the weight, time, and water density at the ambient temperature. To establish a baseline, flow measurement was first carried out without a device. The syringe pump was directly connected to the flowmeter, and the flow rate was calibrated using the direct method.

2.3 Results and Discussion

2.3.1 Flow Meter Calibration

The operation range of the Sensirion flowmeter is 250 nL/min to 7000 nL/min according to the manufacturer. As a result, the flowmeter was calibrated over the same range using the direct method as described in the *Experimental Section*. A water flow was generated by the syringe

pump and the flow rate was measured by the flowmeter and the direct method (weight measurement). No microfluidic device was connected in the setup and stiff tubing was used for connections. Figure 2-2 shows the obtained flow rate as a function of the pumping rate of the syringe pump. The measured flow rate by direct method agreed very well with the pumping rate; the slope of the calibration curve is 1.01. The measured flow rate by the Sensirion flowmeter agreed well with the pumping rate at the lower range (the slope of the calibration curve is 0.97 for values below 5000 nL/min), but it started to deviate from the linear curve when the flow rate was larger than 5000 nL/min. The error bars indicate the standard deviation calculated from all data points collected over 1-5 minutes for each flow rate. The variation in the flowmeter measurement likely resulted from the flow pulsation as discussed later.

2.3.2 Flow Measurement in Devices

The effect of presence of a microfluidic device on the flow rate delivered by a syringe pump was first evaluated. The flow rate was measured using the flowmeter when it was directly connected to the syringe pump as in calibration experiments; the same measurements were then taken when the flowmeter was connected via microfluidic device to the syringe pump as in Figure 2-1. Stiff tubing was used in both experiments. Figure 2-3 shows a comparison in the measured flow rates between these two setups. The error bars in the plots are again the standard deviations. The results suggest that two groups of flow rates are the same within the experimental errors for these two setups in the presence or in the absence of the device, suggesting that a microfluidic device has negligible effects on the flow rate delivered by the syringe pump.

The effect of syringe pumping on flow rate using flexible tubing was next investigated and compared with the case for stiff tubing since stiff tube was expected to maintain pumping pressure. The stiff PEEK tubing that connected the syringe pump and the device in Figure 2-1

was replaced with a flexible silicone tube. Figure 2-4 shows a comparison in the measured flow rates between a setup with stiff tubing and the same setup with flexible tubing. A device was used in both setups. The measured flow rates were lower in the setup with flexible tubing than the one with stiff one, especially in the lower range of the flow rate (less than 5000 nL/min). The slope of the calibration curve is 0.96 for the setup with stiff tubing, which is similar to the Sensirion flowmeter calibration curve in Figure 2-2. However, it was reduced to 0.92 for the setup with flexible tubing, indicating lower flow rates in the devices. Larger standard deviations at the higher range of the flow rates make comparison between the two groups difficult.

This result still indicates a flowmeter is not required if an approximate flow rate suffices. However, an external flowmeter becomes a necessity if one needs to know the accurate flow rate in a device when flexible tubing is used in connecting pumps with devices, especially when a complicated fluid network and the accessories have a possibility to diminish the pumping pressure. The pressure losses in internal viscous flows, often called head loss, could result from channel/tube enlargements and contractions, inlets and exits, valves and other components.[51]

2.3.3 Flow Pulsations

Syringe pumps are extensively used as a pumping method in microfluidic applications. Pump is driven by the linear positive displacement of a syringe plunger resulting from the rotary motion of a stepper motor. The stepping motion is expected to generate flow pulsations.[64, 65] Since the Sensirion flowmeter is very sensitive with rapid response time, it was used to confirm the existence of flow pulsations and study the effects of a microfluidic device and tubing on flow pulsations.

Figure 2-5A shows the temporal profiles of flow rates measured by the flowmeter when it was directly connected to the syringe pump using stiff tubing. Significant flow pulsation was obvious as indicated by the sine wave embedded in white color. When the stiff tubing was

replaced by flexible one, flow pulsation was significantly reduced, presumably due to the damping effects of the tube flexibility on the pumping pressure. When the setup was connected with a device, flow pulsation was further reduced. The effects of the device on flow pulsation are also illustrated in Figure 2-5B, in which a comparison was made between setups with and without a device. Stiff tubing was used in both cases. The results clearly suggest that connection of a microfluidic device with a syringe pump significantly reduced flow pulsations. The flexibility of the thin cover film of the plastic device likely played a role in diminishing pulsations. The results are in the agreement with a study on segmented flows in microfluidic devices.[65]

The effects of the flow rate (from 250 to 7000 nL/min) on flow pulsation were also studied. Representative results at 1000 and 4000 nL/min are shown in Figure 2-5B. Sine waves in white color were added to the temporal profiles to show approximate pulse duration. The average pulse duration over three periods was 31 s for 1000 nL/min while it was 7.6 s for 4000 nL/min. The duration of each pulse is about 2 orders of magnitude longer than the period of the stepping motor in the syringe pump listed in Table 2-1. Longer pulse of the fluid oscillation was likely due to the damping effects of tubing and the device as discussed above.

To confirm the pulse duration mismatch was not a part of the measurement system, two syringe sizes were used that would give different pulse duration due to the change in the stepping motor speed. The syringe with a volume of 100 µL used in all experiments above was replaced with a syringe with a volume of 250µL. Figure 2-5C shows the comparison of temporal profiles of flow rates between two setups using different syringes. The flowmeter was directly connected to the syringe pump without a microfluidic device. Stiff tubing was used in both setups and the flow rate was at 4000 nL/min. Sine waves in white color were also added to the temporal

profiles to show approximate pulse duration. The average pulse duration over three periods was 19.0 s for the 250 µL syringe, which was 2.5 times longer than the pulse duration of 7.6 s for the 100 µL syringe. This ratio is exactly the same as the expected ratio calculated from the parameters listed in Table 2-1. It was inferred from this result that the flowmeter accurately measures flow rates and the observations are true representation of flow pulsations.

2.3.4 Microvalve Testing Using Flowmeter

The valve testing was set up based on the flowmeter evaluation results discussed above. The concept of the valve is shown in Figure 2-6A, which is, to some degree, similar to the elastomer valves developed by Quake and co-workers.[19] The device consists of four layers, including substrate with fluid channels, elastomer, valve layer, and thin film. In Quake's valves, the valve layer contains control channels for pneumatic actuations. In contrast, thermosensitive materials was used in the present valves as indicated. When the heater was turned on, the thermosensitive materials expanded and deflected the elastomer to close the fluid channel as illustrated in Figure 2-6A. Details of microvalve device fabrication and operation are included in chapter 3.

To demonstrate the valving mechanism the microvalve device was connected to the Sensirion flowmeter in a setup similar to Figure 2-1. When the valve is closing, the cross sectional area of the fluid flow decreases, resulting in a change in the flow rate. When the valve is completely closed, the elastomer is entirely deflected to the wall surface, thus the channel is blocked and the flow rate goes to zero. Figure 2-6B shows a temporal profile of the flow rate recording from the Sensirion flowmeter when the valve was open, closed and back to open. The syringe pump was set at 300 nL/min and 400 mW power was supplied to the microheater.

The temporal profile in Figure 2-6B shows the dynamics of valve actuation. Initially the flowmeter recorded the flow rate (300 nL/min) set by the syringe pump. When the valve was

closing (i.e. the heater was turned on), the elastomer was deflected into the channel and the reduction in the flow rate was recorded by the flowmeter. An increase in the flow rate before the reduction likely resulted from the elastomer deflection. The sudden elastomer motion displaced the fluid downstream, resulting in an impulse in the flow velocity. The temporal profile also consisted of a period of negative flow rates, which can be explained by the back pressure. After the elastomer was completely deflected onto the channel wall surface and the flow rate decreased to zero, the inertia of the flow carried the fluid further downstream and a back pressure was developed near the elastomer. This back pressure caused a flow reversal downstream, resulting in a negative flow rate detected by the flowmeter. Once these transient states were completed, the flow reached to the steady state. After the flow in the channel was blocked and continuous zero flow rate was recorded, the valve was opened (i.e., the heater was turned off). The elastomer quickly relaxed to its original shape and flow rate returned to the initial value. However, before reaching the initial flow value there was a slight surge in the flow rate recorded possibly caused by the pressure built up at the valve inlet when the valve was closed.[66] Hence when the valve was opened a momentary/temporal increase in flow was seen which stabilizes with time. This surge effect is clearly illustrated in Figure 2-7 which shows the valve action for an inlet water flow of 300 nL/min. The valve was allowed to stay closed for different times and the corresponding surge in the flow rate after the valve opening is shown. When the valve was kept closed for longer times, higher flow peaks are reached in Figure 2-7, supporting the argument that pressure builds up at the valve inlet due to the principle of syringe pump operation. Higher pressure built-up results in higher magnitude of flow surge once valve opens. The profile with 87-s valve close time uses 190 mW heater input power and the other two (97-s and 183-s) use 66 mW. It can also be noted that for higher powers of valve actuation, here 190

mW case, the initial flowrate increase (prior to valve closing) is higher. It also results in larger reverse flow downstream near the flowmeter once the valve is closed. Faster elastomer deflection results in larger pumping action during valve closing and hence the corresponding negative backpressure near valve exit increases.

Transient characteristics including the sudden surge in the flow rate (before and after valve action) and the negative values were reproducible in many experiments that were performed. The case discussed above illustrates the utility of a flowmeter for studying valve actuation and investigating local flow dynamics.

2.4 Conclusion

A Sensirion flowmeter was evaluated and used to demonstrate a valve actuation mechanism by measuring the real-time flow rates. The flowmeter was calibrated using the direct method, which weighed the amount of fluid collected over a certain period of time. The general agreement between the flow rate set by the syringe pump and the flow rate measured by the flowmeter indicated the reliable accuracy of the flowmeter and that flowmeter is not required for simple setups.

To ensure the flow rate specified by a syringe pump (or those using similar pumping mechanisms) truly represents the actual flow rate in a microfluidic device, stiff tubing should be employed. Effects of stiff or flexible tubing on the flow rate in a microfluidic device was studied and it was found that the use of flexible tubing resulted in a reduction in the flow rate in the device because the pumping pressure was slightly lost due to the stretching of flexible tubing.

In addition, flow pulsation was confirmed to exist when a syringe pump was used. It was found that the degree of flow pulsation is related to the volume of the syringe used in the pump, the stiffness of tubing, the flow rate and the presence of microfluidic devices in the fluid

network. This finding is a significant factor to be considered while setting up the microvalve test station and also since syringe pumps are extensively used in microfluidic applications.

The flow meter was then used to study the valve mechanism of a thermally actuated microvalve. The flowmeter provided detailed flow dynamics associated with the valve actuations.

One drawback of the Sensirion flowmeter is that it must be connected via tubing to a microfluidic device. It would be ideal to have a flow sensor integrated in a device so that it can measure the flow rates at a variety of locations. For instance, flow rates in branched channels of a complicated fluid network must be locally measured in order to know the accurate flow rate in each channel, similarly, presence of valves in a microchannel would need accurate local flow monitoring so as to control the flow effectively. Devices with integrated flow sensors will be useful in applications where accurate flow controls are required.

Table 2-1. Volume of syringes and parameters of syringe pump

Syringe volume	100 µL syringe		250 µL syringe
Flow rate (nL/min)	1000	4000	4000
nL/step	5.315	5.315	13.19
Steps/min	188.2	752.5	303.0
Seconds/step	0.32	0.080	0.20

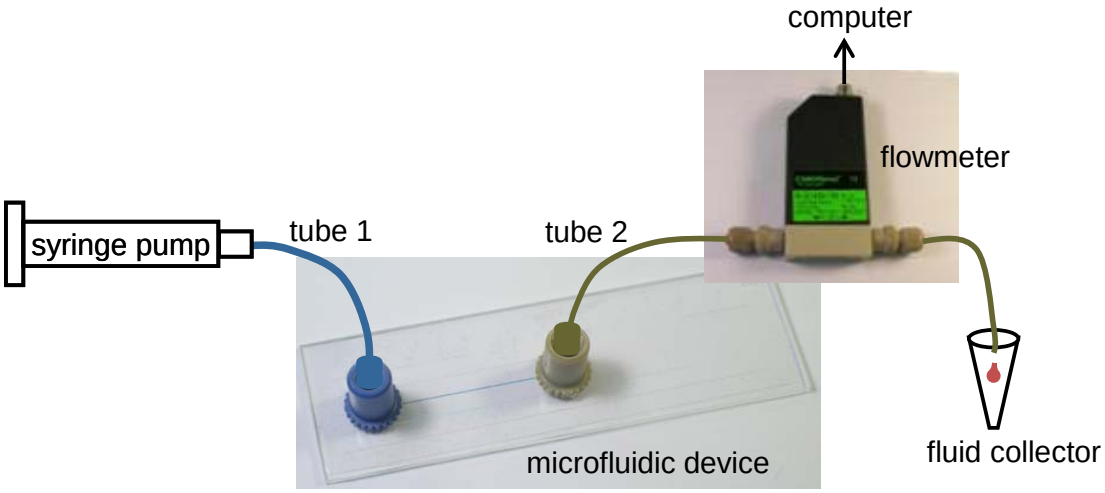

Figure 2-1. Schematic of the experimental setup for this work. A syringe pump was connected via tube 1 to a microfluidic device, which was then connected through tube 2 to a Sensirion flowmeter. The fluid flowing out of the flowmeter was collected for the flow rate calibration

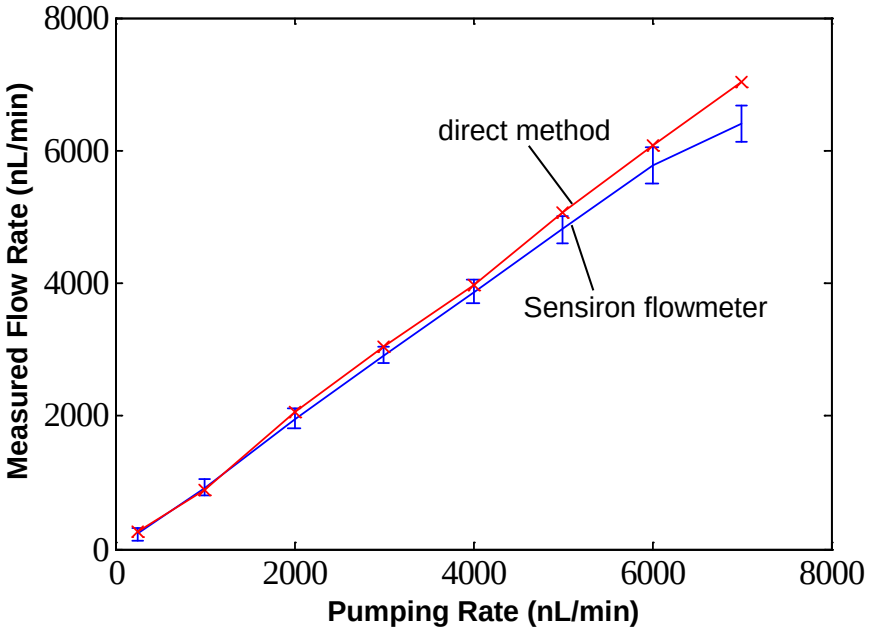

Figure 2-2. Comparison of the flow rates measured by the direct method and the Sensirion flowmeter. The measured flow rates were plotted as a function of the pumping rate of the syringe pump. No microfluidic device was connected between the syringe pump and the flowmeter.

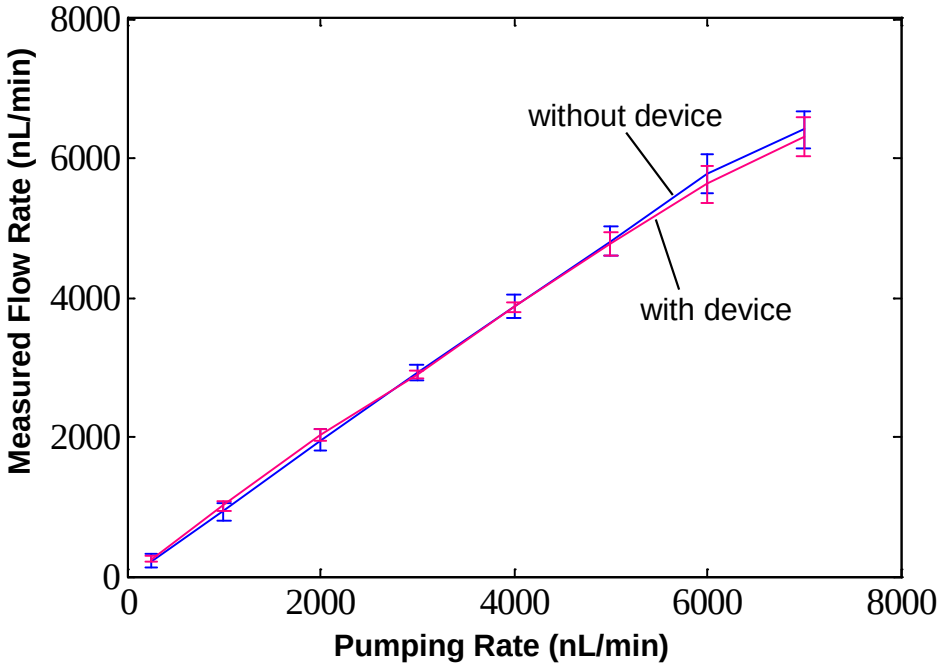

Figure 2-3. Comparison of the flow rates measured by the Sensirion flowmeter in the presence and absence of a microfluidic device. Stiff tubing was used to connect the syringe pump with the device or the flowmeter. The measured flow rates were plotted as a function of the pumping rate of the syringe pump

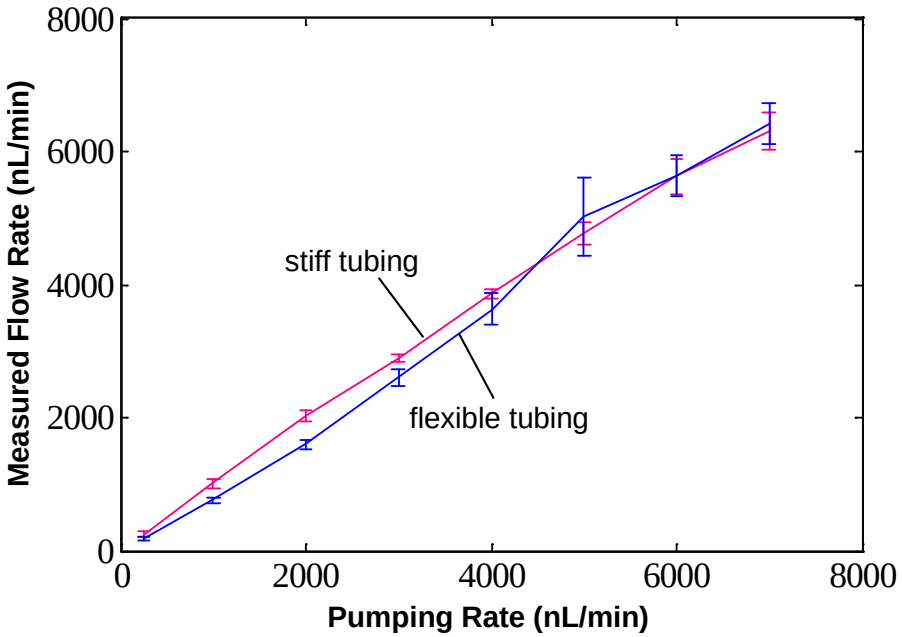

Figure 2-4. Comparison of the flow rates measured by the Sensirion flowmeter in two setups using stiff or flexible tubing. The tubing was used to connect the syringe pump with the microfluidic device as shown in Figure 2-1. The measured flow rates were plotted as a function of the pumping rate of the syringe pump.

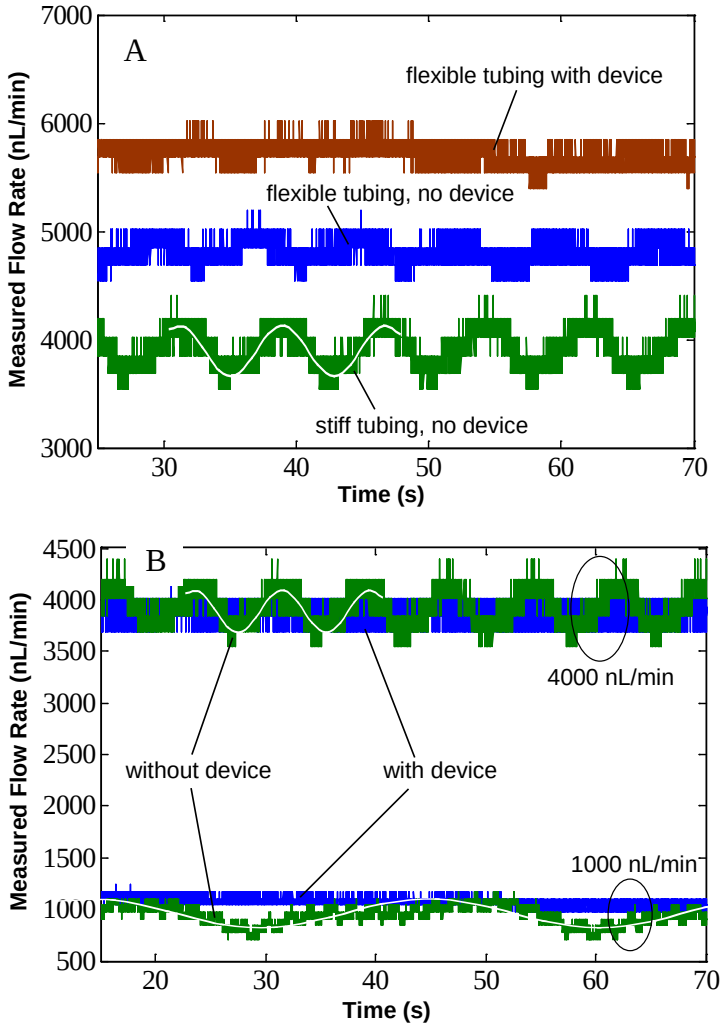

Figure 2-5. Temporal profiles of flow rates measured by the Sensirion flowmeter in different setups. Sine waves in white color were added to show flow pulsations. A) The effects of tubing stiffness on flow pulsations. The flow rate was 4000 nL/min for all of them; the top and middle curves were shifted up by 2000 and 1000 nL/min for clarity. B) The effects of a microfluidic device on flow pulsations. Stiff tubing was used in all setups. The flow rate was either 1000 or 4000 nL/min as indicated. C) The effects of the syringe size on flow pulsations. Stiff tubing was used in both setups (without a microfluidic device). The flow rate was 4000 nL/min while the sizes of syringes were either 100 or 250 µL as indicated.

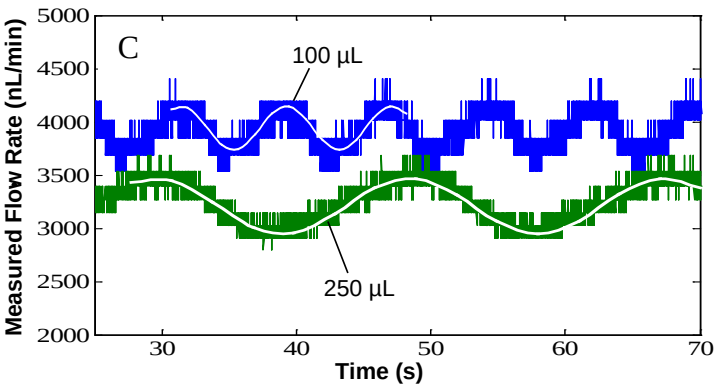

Figure 2-5. Continued.

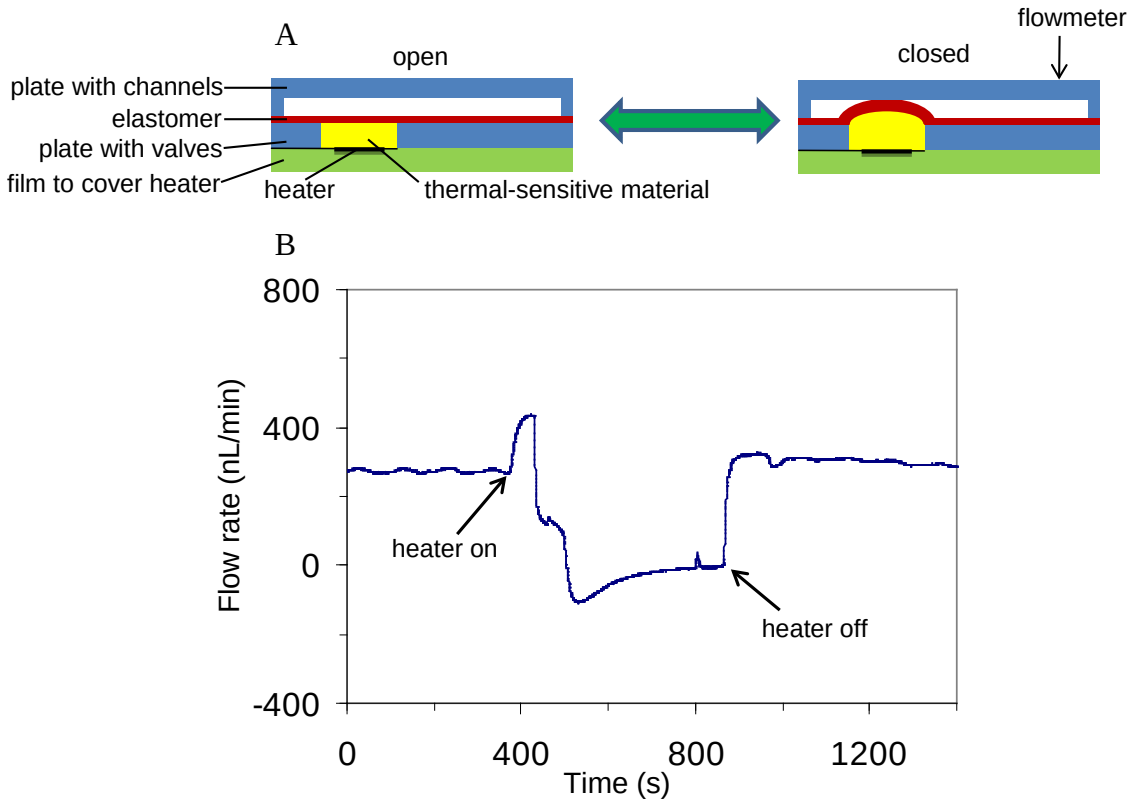

Figure 2-6. Microfluidic valve. A) The valve is actuated by a microheater. The elastomer is deflected to the channel wall when thermo-sensitive material expands. The drawing is not to scale. B) Temporal profile of the flow rate recorded by the Sensirion flowmeter, which was connected downstream to the device. Water was supplied at 300 nL/min by a syringe pump and the valve was then closed, and back to open. 400 mW power was supplied to Minco heater.

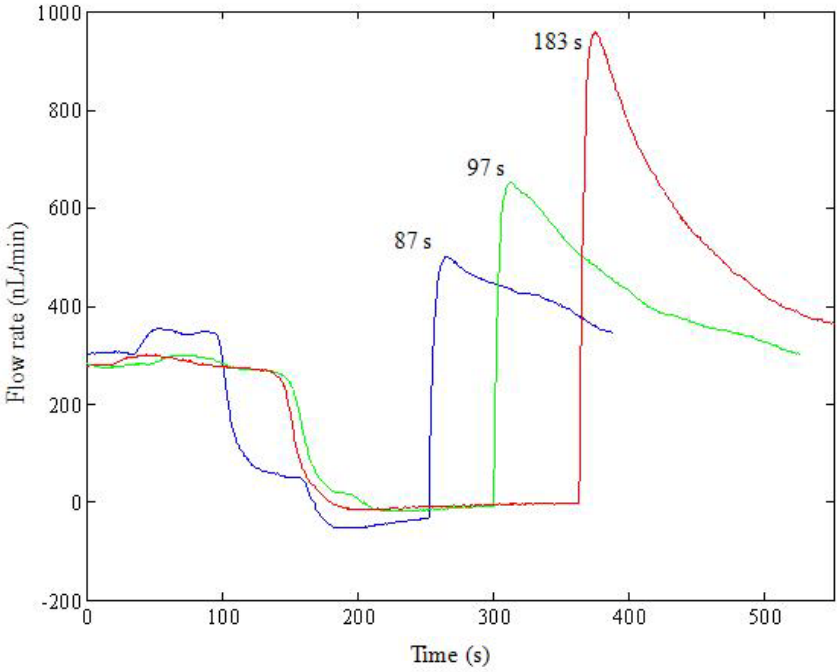

Figure 2-7. Microvalve actuation data recorded by flowmeter showing the local flow dynamics. 300 nL/min of water is supplied by a pump. The valve is kept closed for different times resulting in proportional flow increase once the valve is opened due to pressure built up at valve inlet. 190 mW power is supplied for the 87-second(s) valve close test and 66 mW power is supplied for 97 s and 183 s valve close test.

CHAPTER 3
FABRICATION AND CHARACTERIZATION OF A THERMALLY ACTUATED MICROFLUIDIC VALVE

3.1 Introduction

There are several advantages in microfluidics devices over conventional bench-top instruments. A micro total analysis system (μTAS) promises shorter analysis time, lower reagent consumption with low detection limits.[5] Use of parallel processing enables higher throughput. In addition, plastic microfluidic devices are suitable for mass production lowering the device cost. Overall analysis cost is also reduced. These devices essentially incorporate several critical components such as valves, pumps and mixers to achieve the desired fluidic manipulation necessary for an efficient process control. Inability to develop inexpensive, reliable and portable systems for these components has been a hindrance in the full fledged employment of microfluidic technologies in all the previously predicted application areas.[6] Addressing the problems, this Chapter describes the fabrication and operation of a thermally actuated microvalve. The microvalve is designed to address the above mentioned drawbacks as an improvement over the existing valves reported in the literature. In addition, this chapter describes an 'electric-current' measurement method to study local valve operation. The valve operation was characterized in terms of actuation times, power and flow rates.

3.2 Brief Review of Microvalves

Several microfluidic valves are reported in literature (Chapter 1). Each of these valves is based on different operating principles, material combination and some targeted at specific applications. Earliest work on a complete Lab-on-a-chip device by Harrison et al.[8] made use of electro-osmosis to control sample flow as an EO valve. Valves reported by Quake et al.[19] and Grover et al.[67] consist of pneumatic actuation wherein pneumatic pressure is used to deflect a membrane into a channel. Both normally closed and normally open valves have been made this

way. Beebe et al. have developed pH actuated hydrogel valves which makes use of the surrounding media composition or property such as pH to open or close a channel based on volumetric expansion or contraction of the hydrogel.[41] In-situ polymerized pseudo-gel valves have also been reported by Fan et al.[68] which restricts sample flow. Thermally actuated valves for MEMS based applications have been developed by Tai et al.[35] and a commercially successful valve based on thermal principle is reported by Redwood Inc.[34] for refrigerant flow control. Whitesides et al.[69] developed a simple PDMS membrane valve using quantified mechanical screw rotations to make the valve close. Several other valves have been reported and they are modified versions of the above basic principles.

Although each of these valves demonstrates its functionality, there is still need for a robust, reliable, versatile microfluidic valve which has a wide operating pressure range with zero leakage, low fabrication and operation cost, fabrication ease, faster response times, low power consumption and can be integrated on a large scale. For example, Quake valves[19] making use of multiple PDMS layers are not ideally suited for industrial mass production and the pneumatic connections make the microfluidic device accessories not portable and cumbersome to operate. Valves based on EO flow have leakage problems and several MEMS based valves are based on silicon processing and are not compatible with microfluidic material requirements such as optical clarity for detection. As such, silicon based microfluidic devices are not suitable to realize the predicted advantages of microfluidics as a science of future with promise[17]. Hence a novel microfluidic valve has been proposed and developed which is compatible with industrial fabrication technologies suitable for mass production. The principle of operation for this normally open valve is based on thermal actuation of an elastomeric membrane.

3.3 Principle of Operation

Fabricated microvalve is based on the principle of thermal actuation. When heat is supplied to an incompressible fluid there is volumetric expansion of the fluid due to its temperature rise. This change in volume is used to deflect an elastomeric film into a microfluidic channel to be controlled. The elastomer selected should be of low stiffness and high elasticity so that it can be controlled without excessive heat input and can be used repeatedly. Heat input to the thermally expanding fluid (actuating fluid) is supplied through micro-fabricated heaters. The power supply to these heaters is controlled using printed circuit board (PCB). The concept of using PCB controlled valve actuation will enable large scale integration of these valves for high throughput applications. Figure 3-1 shows the schematic of the multilayer device assembly illustrating the concept of microvalve operation. The nomenclature assigned to each layer is as follows. The microfluidic channel layer is termed ‘channel layer’. The elastomeric film is termed as ‘elastomer film or film’ and the cavity where the thermal fluid is encapsulated is called ‘FC40 well’, named after the commercial grade of the thermal fluid used, and the plastic layer in which it is filled is called ‘valve layer’. The plastic thin film with the heater pattern next to the valve layer is called the ‘heater layer’.

3.4 Experimental Section

3.4.1 Device Fabrication for Microvalve

Plastic microfluidic devices for microvalve were fabricated, as described in the previous section, by injection molding of cyclo-olefin resin (Zeonor 1020R) pellets using a Carver hydraulic press. A CNC milling machine was employed to trim the plastic parts into 1 x 3 in. substrates and drill 2-mm-diameter holes at the channel ends. The holes at channel ends became wells for fluid connections. The device was 1.5 mm thick while all channels in the microfluidic device were 110 µm wide and 45 µm deep. The lengths of channel used for the valve action

study were 25 mm and 47 mm. The cross section of the channels was D-shaped due to isotropic etching of the glass substrate that was used for fabricating the molding master. The substrate was then covered with the elastomeric film and subsequent layers as described in the following sections.

3.4.2 Elastomeric Film

The function of elastomeric film is to deflect itself into the channel during expansion of thermal fluid. The factors in choosing the film materials were based on

- Modulus of elasticity
- Elastomer/membrane thickness
- Bonding with COP Zeonor 1020R

Based on the above factors, following three membrane materials were used for microvalve device fabrication in this study:

- Polydimethylsiloxane (PDMS)
- Polyester (PET) film
- 4 mil (100 µm) thick topas 8007

The method of fabrication based on PET film is described in detail in the following sections.

3.4.3 Polyester (PET) Film

In this section, microvalve device fabrication using PET film is described. The microfluidic substrate (channel layer) milled as described above was cleaned first. For cleaning, the device was submerged in acetone (NF/FCC/EP, F.W. 58.08) and let to sit on a New Brunswick Scientific Shaker (Edison, NJ) for 5 minutes. It was then rinsed in running stream of DI water and dried overnight in the laminar fume hood. Double coated pressure sensitive adhesive (PSA) tape 9019 was obtained from 3M (Minneapolis, MN) in the form of a sample roll. The PSA tape has a Polyester (PET) base film of 13 µm thickness coated on both sides with 8.4 µm thick adhesive 300. Thus the total film thickness is 29.8 µm. Adhesive 300 is an acrylic

based medium-firm adhesive suited for low surface energy (LSE) plastics like cyclo olefin polymers. In order to transfer the PET film over channel layer the kraft liner from one side of adhesive 300 was removed. Hand held rubber Squeegee was used to manually laminate the PET film over the device. The film was laminated from one end to the other longitudinally to minimize air entrapment and thus maximize bonding area. This process was carried out in the clean air environment of the laminar hood. The squeegee was firmly used over the other side of the film on the liner for 3-4 times to ensure firm contact with the channel layer. The two layer assembly was then left for 24 hours to allow the bond strength to increase.

Next, the layer of microvalve to hold the thermal fluid was integrated with the previously made two layers. This third layer called the 'valve layer' was made of 250 µm thick Zeonor 1020R Cyclo-olefin polymer film from PLITEK (Des Plaines, IN). The film was cut into 1 x 3 inch size and has 2 mm holes at locations where valve actuation is desired. The hole/cavity was for filling the thermal fluid. The valve-layer was cleaned with the same method as the channel layer using acetone and DI water rinse and left to dry overnight in a laminar hood. The clean and dry valve-layer was then assembled with the previously assembled two layers of channel layer and PET film. For the same, the remaining liner on the PET film (opposite to channel side) is peeled off followed by valve-layer assembly. The valve-layer was visually aligned such that the microfluidic channels runs below the centre of thermal fluid cavity and laminated over the PET film with exposed adhesive 300. Lamination was carried out using a J-type Gundlach rubber roller (Belleville, IL) with firm manual pressure to ensure maximum surface contact and minimum air entrapment. Roller was run over the three layer device assembly for 3-4 times. Assembly was performed in laminar hood to ensure no dirt/dust or foreign particles affect interlayer bonding. The assembled device was then left in the laminar hood for at least 2 hours to

increase the adhesive bond strength. The thermal cavity, referred to as FC40 well, was temporarily sealed using a Costar thermowell sealer polyethylene tape from Corning (Corning, NY) to prevent dust from entering. The cover was removed before the next layer is bonded to the device. The three layer assembly was then bonded with a 250 µm thick Zeonor 1020R film to seal the FC40 well. The cavity was subsequently filled with Fluorinert FC40 from 3M (Minneapolis, MN) using vacuum.

3.4.4 Microheaters

Resistive Microheaters were fabricated by sputter deposition of gold on plastic films. Heaters are serpentine Au resistors with specific thickness. The serpentine heater was designed in AutoCAD and the pattern was printed on a Transparency using a high resolution printer (5080 dpi from Pageworks, Cambridge, MA). The transparency was used as a photomask to photolithographically pattern the gold film deposited on plastic. 250 µm thick Zeonor 1020R film was cut to 4 x 2 inch sizes and rinsed with acetone and DI water and dried overnight in a laminar hood. Kurt Lesker CMS-18 Multi Target Sputter Deposition tool (Pittsburgh, PA) was used to deposit 1000 Å thick Au film on the cleaned 1020R 250 µm film. The deposition rate was 5 Å/sec and the time for deposition is 200 sec. After deposition of the Au film, positive photoresist Microposit S1813 from Shipley (Marlborough, MA) was spun on the Au coating in two steps. In the first step, the spinner was set at 1000 rpm for 15 sec followed by 5000 rpm for 50 sec. The Laurell spinner WS-400A-6NPP/Lite (North Wales, PA) was set at an acceleration of #15 (1560 rpm/sec) and the corresponding thickness of PR was 1.8 µm. The PR was then prebaked at room temperature for 24 hours. Karl Suss MA6 Contact Mask Aligner (Germany) was used to pattern the PR through the transparency mask. The PR was exposed at 365 nm for 20 seconds. The exposed PR was then developed using AZ 300 MIF for about 40 to 50 seconds followed by DI water rinse and Nitrogen stream dry. The developed Au pattern was then

hardbaked at room temperature for 24 hours. Gold etchant TFA from Transene Company Inc. (Danvers, MA) was used to etch the patterned Au. The film with Au was submerged in the etched solution for 40 seconds to obtain the serpentine Au resistive heaters. The etched Au pattern on the plastic film was finally rinsed in acetone followed by DI water. It is then left in laminar hood to dry overnight or dried using a Nitrogen stream.

The resistive heater pattern has provision for a hole to be drilled so that the thermal fluid Fluorinert FC40 can be filled. The hole was drilled in the heater film using a 100 µm diamter drill bit MD-010-2FL from Cutting edge technologies (Plymouth, MA). The CNC milling machine was used to drill the hole and the alignment was done visually. The heater is kept face-up while drilling so that the Au side of the heater film has smoother finish. Once the holes were drilled the heater film was cut along the outline of the heater. It was then rinsed with DI water and dried using filtered dry air or Nitrogen stream. Alternately, it can be left to dry in laminar hood. The dried heater film with the patterned Au heater and the filling hole was then assembled over valve layer in the previously made three layer microvalve device. The heater layer was solvent bonded on top of the FC40 well using decalin[70] from Fischer scientific (Fair Lawn, NJ). The heater layer was stamped over 0.1 mL of decalin placed on a 1 x 3 in. microscope slide and transferred on top of the FC40 well. Alignment was done visually such that the serpentine heater pattern was within the FC40 well cavity. Uniform hand pressure was sufficient to ensure enough surface contact with minimal air bubbles. The assembly was then heated at 60^{o}C for 20 min. to complete the solvent bonding.

3.4.5 Thermal Fluid

Once the heater layer was bonded, the FC40 well in valve-layer is then filled with Fluorinert FC40. 10 ml of Fluorinert was taken in a 200 ml Pyrex glass beaker and the microvalve device was immersed in the liquid such that the filling hole was about 1-2 mm below

the liquid meniscus level. This assembly was placed in a vacuum chamber which was at a 20 in. Hg vacuum pressure. The assembly was subjected to vacuum for 30 seconds followed by vacuum release and then again for 4 minutes followed by vacuum release. The filled cavity was then sealed with a drop of RBC2001 epoxy (Warwick, RI) or conductive epoxy from Chemtronics (Kennesaw, GA) if needed for fluorescence experiments. The epoxy was cured at room temperature overnight. The filled cavity could also be sealed by solvent bonding another layer of 100 μm thick Zeonor 1020R using decalin and letting it cure at room temperature overnight. Upchurch Nanoport fitting (Oak Harbour, WA) was then connected to the inlet of the microfluidic channel with valve on it using RBC2001 epoxy. Heater connecting wires were bonded on the heater traces using conductive epoxy from Chemtronics and let to cure overnight. Figure 3-2 shows the multilayer microvalve device.

3.4.6 Valve Characterization

3.4.6.1 Electric-current method

Valve testing for actuation and proof of concept were performed by measuring channel conductivity[71]. A Microfluidic channel with a valve was filled with either 1M or 0.1M NaCl solution and the change in current through it was measured as a function of time for a specific applied power to heater. Platinum electrodes, 0.3 mm in diameter, 99.9% purity from Alfa Aesar (Ward Hill, MA) were immersed into the inlet and outlet wells of the channel to supply a constant voltage. The current through this circuit was measured using an external series resistance of 56KΩ. The setup for principle of 'Electric-Current method' based on channel conductivity measurement is shown in Figure 3-3.

A Labview program was written to automate the data measurement and analysis process. Multifunctional DAQ card NI-PCI 6229 was procured from National Instruments (Austin, TX) along with SCC68 68 pin connector block and SCC-TC thermocouple signal processing module.

The DAQ card and the connector block were used to measure voltage and also to supply DC voltage for electric-current method of valve actuation. The signal conditioning module was also used to measure temperature through the thermocouple attached near FC40well during valve action. Data acquisition was set at 10 Hz sampling. Figure 3-4 shows the Labview user interface for the data acquisition. A supply voltage of 8V DC was used for current-method of measurement. For a 25 mm long channel the resistivity of a 0.1M salt solution was determined experimentally to be 1.899 Ωm corresponding to a channel resistance of 13 MΩ. The connected series resistance of 56 KΩ is 0.4% of the channel resistance. Supply voltage to heater is given by DC power supply from Agilent (Santa Clara, CA).

The setup discussed above is for valve characterization when hydrostatic head was used as a pumping mechanism. In order to test valve for higher inlet pressures either a syringe pump or a hydrostatic head column was used. A UMP-II syringe pump from World Precision Instruments, Inc. (Sarasota, FL.) was controlled by a Micro4 controller. When using a syringe pump an Upchurch T fitting P-712 was used to connect the Pt electrode to the tubing. An Upchurch PEEK tube with 100 μm ID and 1.57 mm OD was used to connect the syringe to the device. A 100-μl gastight Hamilton 1710LT syringe (Reno, Nevada) was used for the reagent delivery. The reagents used in the experiments were 1M or 0.1M NaCl solution.

3.4.6.2 Temperature measurement

Type K thermocouples (TC) from Omega (Stamford, CT) were used to measure temperature in the valve area during valve actuation. A 76 μm diameter 5SC-TT-K-40-36 TC was used to measure temperature outside the heater film on the valve assembly. The TC was insulated with four 1x1 cm kapton tapes. To calibrate the temperature inside the channel, Chal 002, 50 μm diameter, K type TC was inserted into a channel and FC40 during valve action.

3.4.6.3 Fluorescence measurement

Rhodamine B (0.1 mM , 20 mM carbonate buffer) was used to study valve action by measuring its fluorescence during valve action. The microvalve device was placed in the sample stage of the inverted microscope (IX51, Olympus, America Inc., Melville, NY), which was equipped with a 75W Xenon lamp (U-LH75X). A 10x objective lens (Olympus) with a numerical aperture of 0.3 and a working distance of 10 mm was used. The light passes through an excitation filter (HQ480/40, Chroma Technology, Rockingham, VT), a beam splitter, and an emission filter (HQ630/60m, Chroma Technology, for Rhodamine B (special blue filter set)). The channel is filled with the fluorescent solution and images were acquired by scientific-grade CCD digital camera C4742-80-12AG from Hamamatsu (Bridgewater, NJ). The camera exposure rate is set at 21ms. Image data acquisition and analysis was done using Wasabi software from Hamamatsu. In certain cases, the channel walls were coated to reduce residual fluorescent dye adhesion to walls and surfaces. The coating was performed as follows: channels were first rinsed with DI water or 1x tris-HCl tricine buffer. They were then filled with 2% HEC , 1% BSA, 1x tris-HCl tricine buffer and let to stay for 30 to 60 min, followed by DI water or buffer rinse.

3.5 Results and Discussion

3.5.1 Device Fabrication

The first challenge in developing the microvalve was to fabricate the multilayer device wherein different layers had to be bonded to form a cohesive unit. Different elastomer materials were tried including PDMS, PET film and 4 mil cyclo olefin copolymer topas film. PDMS elastomer film, although satisfactory for bonding channel layer with elastomer, was not sufficient to retain the thermal fluid. The possible reason was improper adhesion between the PDMS elastomer film and the valve layer. 4 mil topas film, although, enabled fabrication of a complete microvalve device, was not an ideal elastomer material choice owing to its higher thickness of

100 μm compared to channel cross section, very low elastic elongation and high brittleness. Table 3-1 shows the comparative modulus of elasticity of the three membrane materials studied in this work. The successful microvalve device was achieved using PET film which showed good bonding with Zeonor 1020 R layers (channel and valve layer) owing to its low-surface-energy (LSE) plastic bonding properties. Polyester film has very good solvent resistance and the PSA maintains its properties over a wide range of temperature. It can be operated up to 121^{o}C for few hours and can be used up to 82^{o}C for weeks. Manual squeegee PET application was sufficient to bond layers with minimal air entrapment for operation of microvalve.

3.5.1.1 Heater fabrication and integration

The sputter deposition of 5Å/sec for 200 sec was intended to give a 1000 Å thick Au heater film. The mean resistance for a sample size of 36 resistive patterns was 222 Ω with a standard deviation of 12 Ω. Solvent bonding of the heater layer over the valve-layer using decalin was irreversible and was found to retain its bond during repeated valve actuation cycles. The temperature of the thermal fluid during valve operation was dependent on the power input to the heater. The maximum power that could be supplied to the heater was limited by the Tg (glass transition temperature) of the heater layer (250 μm plastic film), however, power less than the maximum allowed was sufficient for valve actuation.

3.5.1.2 Fluorinert encapsulation

Fluorinert encapsulation is the filling of thermal fluid in the FC40 well. Vacuum filling was the method used for encapsulation. Based on visual inspection the size of air bubble (diameter) as seen in Figure 3-2 from heater top is reproducibly at around 25% of the FC40-well diameter which corresponds to 6% of cavity volume. The air bubble is assumed to be a cylinder with height equal to valve layer thickness i.e., 250 μm. The PET film was not permeable to FC40 as observed for devices which retained FC40 for months. FC40 was stable and did not have any

adverse reaction with the PET film, Zeonor plastic and sealing epoxy. Sealing of the filling hole using epoxy or solvent bonding another plastic film was successful as it retained the thermal fluid over the course of experiments. Solvent bonding method of sealing the hole although adds to the device complexity but helps to maintain the optical clarity of the valve region. This in turn helps monitor FC40 well for Fluorinert expansion, leakage and local fluid flow during valve close or open state. Additional details are mentioned in the next section.

3.5.2 Valve Characterization

3.5.2.1 Cyclic valve operation

The electric-current method was used for most of the valve characterization experiments. Here, current through the channel was measured and the degree of valve action governs the magnitude of this current. Figure 3-5 shows the cyclic valve actuation for the microfluidic valve with PET elastomer film. Au heaters were used to heat the fluid. A power of 58 mW was supplied to the heater and the corresponding rise in temperature was measured across the heater film on the exposed side.

The microfluidic device was supplied with a 9.5 mm hydrostatic head of 1 M NaCl salt solution. It can be seen that the channel conductivity reduces with increase in temperature which agrees with the physics of the microvalve actuation. As the temperature of the thermal fluid increases the membrane deflects into the channel. This results in a reduction in local cross sectional area thereby increasing the channel resistance. Further, the increase in channel resistance causes the reduction in the current and the corresponding voltage drop across the series resistance. This voltage drop was measured and recorded by Labview program using the NI data acquisition system. Cyclic valve actuation is thus demonstrated for a specific pressure input to fluid. It also shows the repeatability of valve operation. Consecutive cycles show a reduction in the actuation time which can be explained based on the thermal diffusivity of FC40

since consequent cycles will need less power to heat the thermal fluid to the actuation temperature.

3.5.2.2 Actuation time

The valve actuation time is defined as the time when the heater power is switched on to the time the voltage reduces to a value less than 3100 μV and holds to that value for ~5 sec. Figure 3-6 shows the variation of this valve actuation time for different input power to heater. The driving pressure for the 1 M NaCl to flow was supplied by the hydrostatic head of 9.5 mm. Figure 3-5 and Figure 3-6 are recordings for the same microvalve device. It is seen that the valve can be operated over a wide range of input power to heater. Depending on the input power, the valve actuation time varies. With increase in power, initially there is a considerable reduction in the actuation time as can be expected since higher power results in higher temperatures in shorter times. However, beyond a power value of 50 mW the actuation time reaches a plateau probably because a saturation heat input value has been reached and beyond which the actuation time or the membrane deflection time constant does not vary significantly. For each power value, except for the lowest power, 6 to 8 valve tests were conducted to obtain the error bars. Error bars are at one standard deviation. For the 36 mW power input, of the three tests, only one showed complete actuation remaining two had partial valve action in an hour.

3.5.2.3 Operating temperature

Being a thermally actuated microfluidic valve, one of the most critical operating parameters is the operation temperature. It is important to characterize the operating temperature at various locations in the microvalve device. The temperature of thermal fluid in the FC40 well determines the actual operating parameter. The temperature of the fluid in the microchannel is another important data of interest to end user. Since enzymes denature at a temperature in excess of $50^{o}C$[72] it is very important for the microvalve to operate within this cut-off value.Figure 3-7A

shows the temperature data measured for thermocouple in the FC40 well. Two cycles of 2 min heater operation are shown. The temperature measured in FC40 well is compared with the temperature measured on the exposed surface of the heater film. The outside thermocouple has a stack of four 1 cm x 1cm kapton tape insulation. The temperature in FC40 well is higher because of direct contact with the heater. Figure 3-7B compares temperature on the exposed surface of the heater layer with the temperature in microchannel. The thermocouple in the channel was placed at a distance of 0.2 mm from the FC40 well edge. The temperature in channel is lower than outside temperature due to insulation provided by the elastomer, radial heat conduction across the device and heat loss to the ambient. The locations of thermocouple in the device microvalve are illustrated in Figure 3-7C.

Thermal characterization of the microvalve involves a plot of temperature as a function of power. Figure 3-8 shows the relationship between temperature and power supplied. The error bars are the standard deviations. For the channel temperature measurement, the thermocouple was placed at a distance of 0.8 mm and 2 mm from the FC40 well edge. As explained above, the temperature in the FC40 well is higher than that in the channels. The maximum operational power is constrained such that the maximum temperature in the microvalve device is less than the lowest Tg of the device components. Since the PET film can withstand temperatures up to 121^{o}C, the restricting parameter is the Tg of the 1020R Zeonor film which is 105^{o}C. The power was limited to 80 mW for the 1000 Å Au heater. Above this power distortion in the heater pattern could be seen, on repeated uses, in the form of wrinkles which are indicative of excessive thermal stresses in the Au-plastic interface. The channel temperature corresponding to the maximum operating power was found to be less than 45^{o}C. Thus, the power required for valve operation and the corresponding heater and component temperatures were found to be within the

critical limits of device integrity without affecting end user applications. The minimum temperature difference required to actuate the valve based on thermal fluid expansion, (Equation 3-1), was found to be 8.7^{o}C. The temperature measured by thermocouple in FC40 well shows that actuation is achieved for temperature difference ranging from 25^{o}C to 55^{o}C. The probable reasons for difference include heat losses through conduction to the substrate material, convection of heat from the exposed device surface and possible deflection of heater film. The presence of an air bubble approximately covering 6% of the thermal fluid well volume also contributes to this difference. The bubble size was approximately less than 500 μm in diameter corresponding to 6% of FC40 well volume. However, the theoretical temperature difference needed corresponding to this reduction in FC40 volume was 9.3^{o}C. Hence other factors play a greater role. The relationship between the volumetric expansion and temperature can be described by

$$\frac{dV}{dT}\frac{1}{V} = \alpha \quad , \tag{3-1}$$

where α is 0.0012 cm^3/ (cm^3 ^{o}C) the volumetric coefficient of thermal expansion of FC40. dV and dT are the change in volume and temperature. The change in volume is equal to channel volume in valve region equal to 8.2e-6 cm^3. V is the total volume of FC40 well 785.4e-6 cm^3. Corresponding minimum dT is 8.7^{o}C.

3.5.2.4 Valve operation with liquid pressure: pumping and hydrostatic head

From the practical application perspective, the valve actuation is tested for syringe pumped flow and with hydrostatic head. The syringe pump was used to supply flow at a constant flow rate or a liquid column at the inlet was used for hydrostatic head. Figure 3-9A and B show a comparative valve action plot for a 300 nL/min (1.2 mm/sec flow velocity) pumped flow at two different heater input powers. 1M NaCl solution is used as the reagent. With increase in input

power, the actuation time for valve to close decreases and the time for valve to open increases. The results are in agreement with the physics; with increase in heater input power, the temperature at which valve actuates is reached faster. However it will take longer time to cool down and open the valve due to the thermal diffusivity of the FC40 thermal fluid. Thus there should be an optimum valve operation power depending on the time constants desired. Addressing the above claim, Figure 3-9C summarizes the actuation times of the valve to open and close as a function of heater input power.

Syringe pump is a constant flow source as a result during valve action pressure will rise locally near the valve region.[66] There are two outcomes of this fact. Firstly, such an increase in pressure locally is not controlled hence the pressures at times were found to delaminate the well region elastomer film. As a consequence, this was found to affect the device performance. Secondly, to monitor this pressure rise and to completely characterize valve using a syringe pump a pressure sensor needs to be connected upstream between the syringe pump and valve to monitor the pressure in microfluidic channel during operation.

As an alternate method to characterize valve action with positive applied fluid pressure hydrostatic head was used. Hydrostatic head was designed here to be a constant pressure source as a result uncontrolled pressure rise at the valve region was avoided. The flow rate through the microfluidic channel corresponding to the head was calculated using the Hagen-Poiseuille flow (Equation 3-2)[73] which considers the head loss due to viscous effect of the fluid flow. The flow rate Q can be calculated using the equation:

$$Q = \frac{\pi \Delta P D_h^4}{128 \mu L}, \tag{3-2}$$

where A is the cross sectional area 4.1e-5 cm^2 and P is the perimeter 1.8e-2 cm. The dynamic viscosity is represented by μ 8.9e-7 Pa-s for 0.1M NaCl and L is the channel length 4.7 cm. The

hydrostatic pressure difference across the channel is given by ΔP in Pa as shown in Table 3-2. Hydraulic diameter, D_h can be defined by:

$$D_h = \frac{2A}{P} \tag{3-3}$$

Figure 3-10 shows a plot of channel conductivity as a function of time for values of pressure heads. The heads are given in 'mm' of 0.1 M NaCl solution. The power is maintained constant at a value of 55 mW. It is observed that the actuation time for valve to close increases with increase in inlet pressure. Longer time was needed for higher heat accumulation for valve to actuate and counter the increase in inlet pressure. Table 3-2 lists the pressure and flow rate values corresponding to the hydrostatic heads for a 47 mm long microfluidic channel used for the valve test. The density was measured using Fischer accu-124 analytical balance (with an accuracy of 0.1 mg) to be 990 Kg/m^3 which is similar to the value of 1001 Kg/m^3 calculated based on the data published in the NIST scientific and technical database for 25^oC.

3.5.2.5 Fluorescence measurement

Rhodamine B (0.1 mM in 20 mM carbonate buffer) was used as the fluorescent dye for the valve action imaging experiments. The valve area under the FC40 well was imaged using the CCD camera controlled by Wasabi software GUI. The channel was surface coated and filled with Rhodamine B prior to valve action. The coating described in the experimental section helps reduce the residual adhesion of dye to channel wall surfaces. Figure 3-11 shows fluorescence images of the valve area before and after valve actuation. The reduction in intensity of dye in the FC40 well region indicates valve action. On supplying a power of 68 mW to heater, the PET film deflects into the microfluidic channel and displaces the fluorescent dye thus resulting in an intensity reduction. The higher intensity near the longitudinal channel edge is probably due to displacement of PSA during actuation. The PSA on PET film would be displaced towards the

pivot point of elastomer deflection which is the channel edge. Fluorescent imaging thus demonstrates the concept of valve operation.

3.6 Conclusion

This chapter reports the fabrication and testing of a thermally actuated microvalve for a plastic microfluidic device. Multilayer device fabrication involves bonding several layers together. The elastomeric film's elastic properties and its ability to be bonded to the microfluidic channel were found to be critical for successful device fabrication. The device has been fabricated and the concept was demonstrated in terms of valve actuation using an 'electric-current' method. The valve actuation times were found to be less than 10 sec, however, consistent repeatability needs to be improved. The operation temperature is within the maximum allowable temperature the components of microvalve device can withstand. Valve actuation was achieved over a range of heater input powers from 36 mW to 80 mW. For consistent actuation higher than 45 mW is desirable. The maximum number of times the valve could be used varied depending on the pressure source used. For a input head of 9.5 mm the valve was found to operate for 50 actuations. The valve was also integrated to a printed circuit board (PCB) (Figure 3-12) to control the power supply to the heater thus setting the stage for next level of device fabrication addressing large scale integration.

The PET film used for valve test demonstration has pressure sensitive adhesive on either side. The adhesive was found to exhibit strong bonding with plastic and was sufficient to hold the device intact enabling valve testing. However, it was found that on repeated valve actuations the glue would accumulate near the channel edge which is a hindrance to realize large number of cyclic valve operation. Also, presence of glue makes it necessary for the channel surface to be pretreated if it is to be used for real life sample manipulation.

The valve has been shown to operate with syringe pumped flows or under hydrostatic inlet heads. The valve relaxation time or the time for valve to switch off once the heat input is stopped was found to be dependent on heater power and for subsequent cycles dependent on the inlet flow rate. Presence of adhesive on elastomer sometimes resulted in sticking effect causing hysteresis in valve operation.

The ‘electric-current’ method of measurement gives a very high response time for local valve actuation. However, it has an inherent disadvantage since current will flow through any conducting path. Although, the elastomer, adhesive and plastic were found to be not conductive when tested separately, even a thin layer of conductive solution would shunt the electric circuit. Thus controlling current leakage path was difficult in some cases. Also, the electric-current method does not give the actual flow rate of the reagent. However, the methods ability to give fast, local action outweighs its negatives. More so, similar current method have been used previously.[40, 71] In summary, the microfluidic valve demonstrated here is the first step towards realizing a reliable valve whose fabrication will suite mass production manufacturing technology and large scale integration.

Table 3-1. Elastomer film properties

Elastomer film	Modulus of elasticity, Kpa	Tensile strength, Kpa	Elongation %	Solvent resistant	Operating temperature range ^{o}C
Poly dimethyl siloxane (PDMS)	750 [74]	6.2×10^6	100	Swells with non-polar organic fluids [75]	-55 to 200
Polyester	(2.8 to 3.1) x 10^6	5.5 to 7.5 x 10^6	50 -150	Medium to Low solvent resistance	-40 to 82 (long-term). -40 to 121 (short term)
Cyclo olefin copolymer Topas 8007	2.6×10^6	63×10^6	10	Attacked by non-polar organic solvents	Heat deflection temperature = 75

Table 3-2. Hydrostatic heads and flow rates

Hydrostatic head in mm	Pressure in Pa	Flow rate in nL/min
40	388	890
70	680	1577
100	971	2225
135	1311	3004
215	2087	4748

The inlet pressure and flow rate corresponding to the applied hydrostatic heads are tabulated. The length of microfluidic channel used is 47 mm.

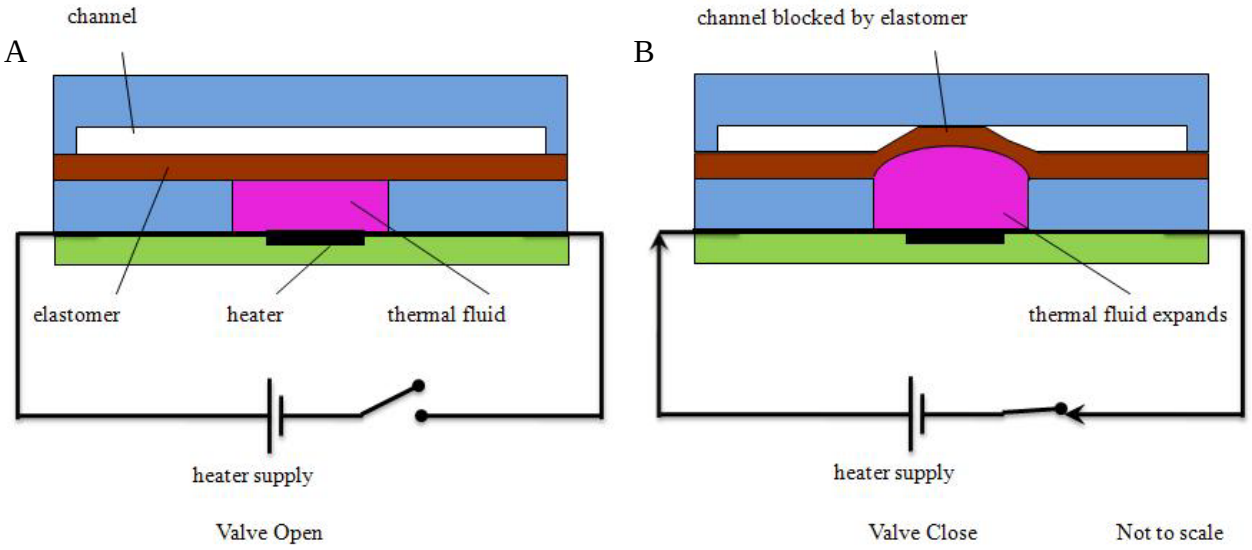

Figure 3-1. Schematic of the microfluidic valve concept based on thermal actuation principle. A) Valve open B) Valve closed. Heat supplied to an expanding thermal fluid causes an elastomer film to deflect into the channel and regulate the flow.

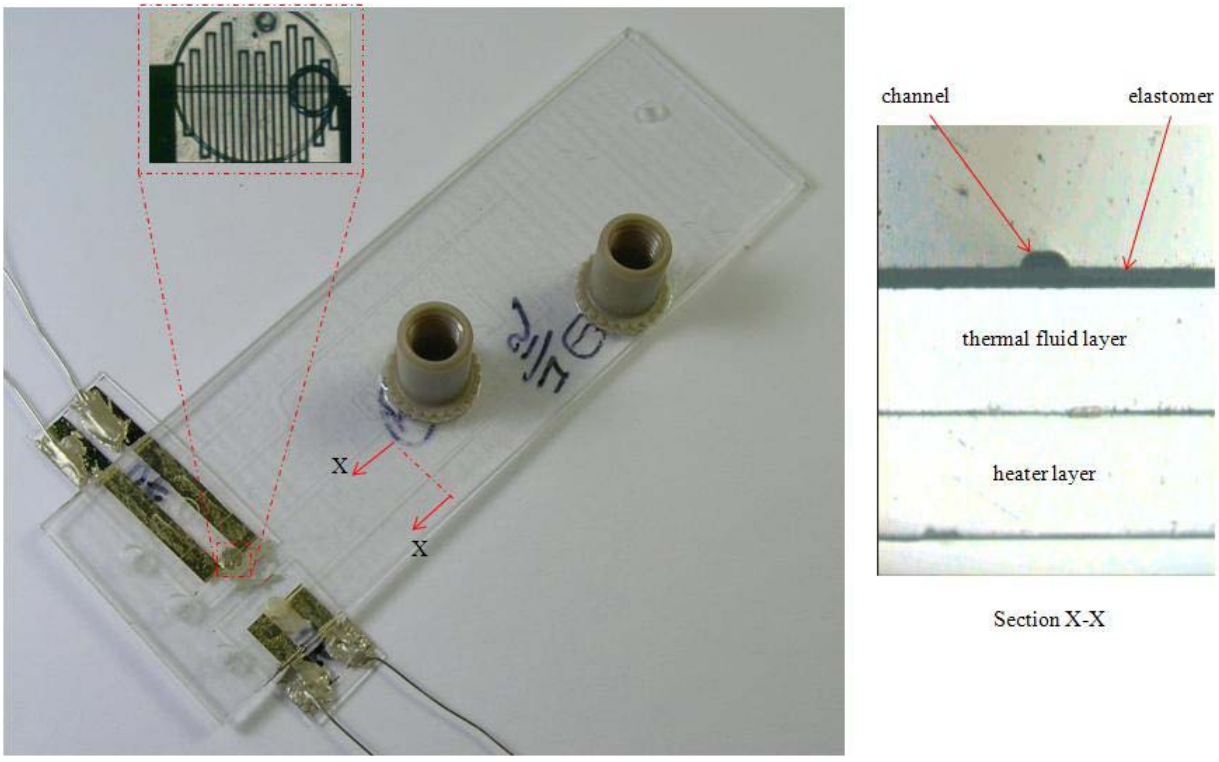

Figure 3-2. Multilayer microvalve device. Inset: FC40 well filled with Fluorinert FC40. The serpentine Au resistive heaters are also seen with the sealed filling hole. Section X-X shows the actual cross section of the multilayer device made using Lapping films with grain sizes 5 µm, 3 µm, 1 µm and 0.1 µm obtained from Thorlabs (Newton ,NJ)

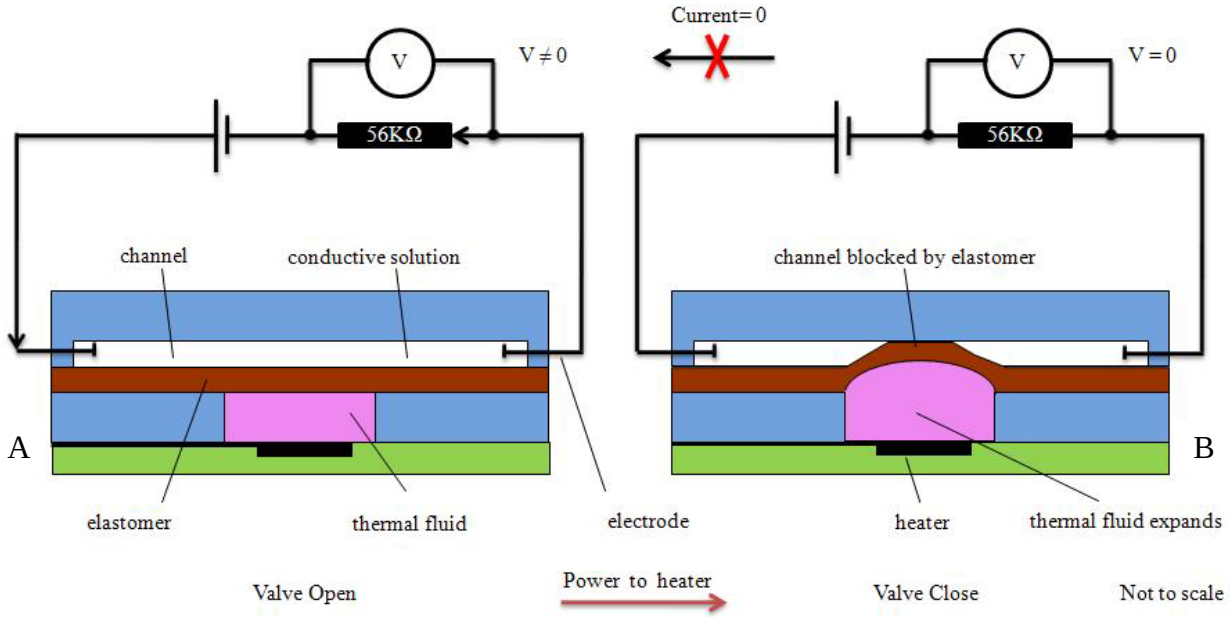

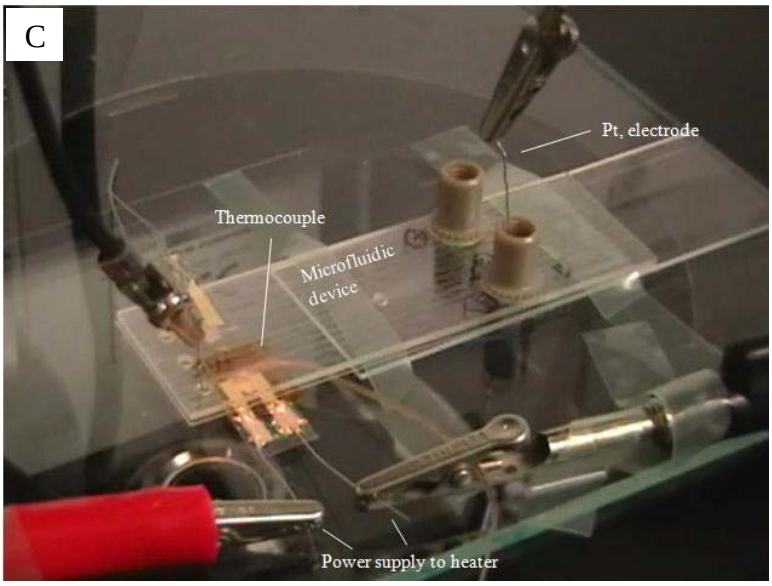

Figure 3-3. Electric-current method to study valve actuation. A) Valve is in open position. The channel is filled with a conductive solution which allows current to flow through it. B) When power is supplied to the heater, the valve goes to closed position blocking the channel. The corresponding current through the channel, thus, goes to zero. C)Actual experimental setup showing the microvalve device connected to a power supply. Pt electrodes are used for electric-current measurement.

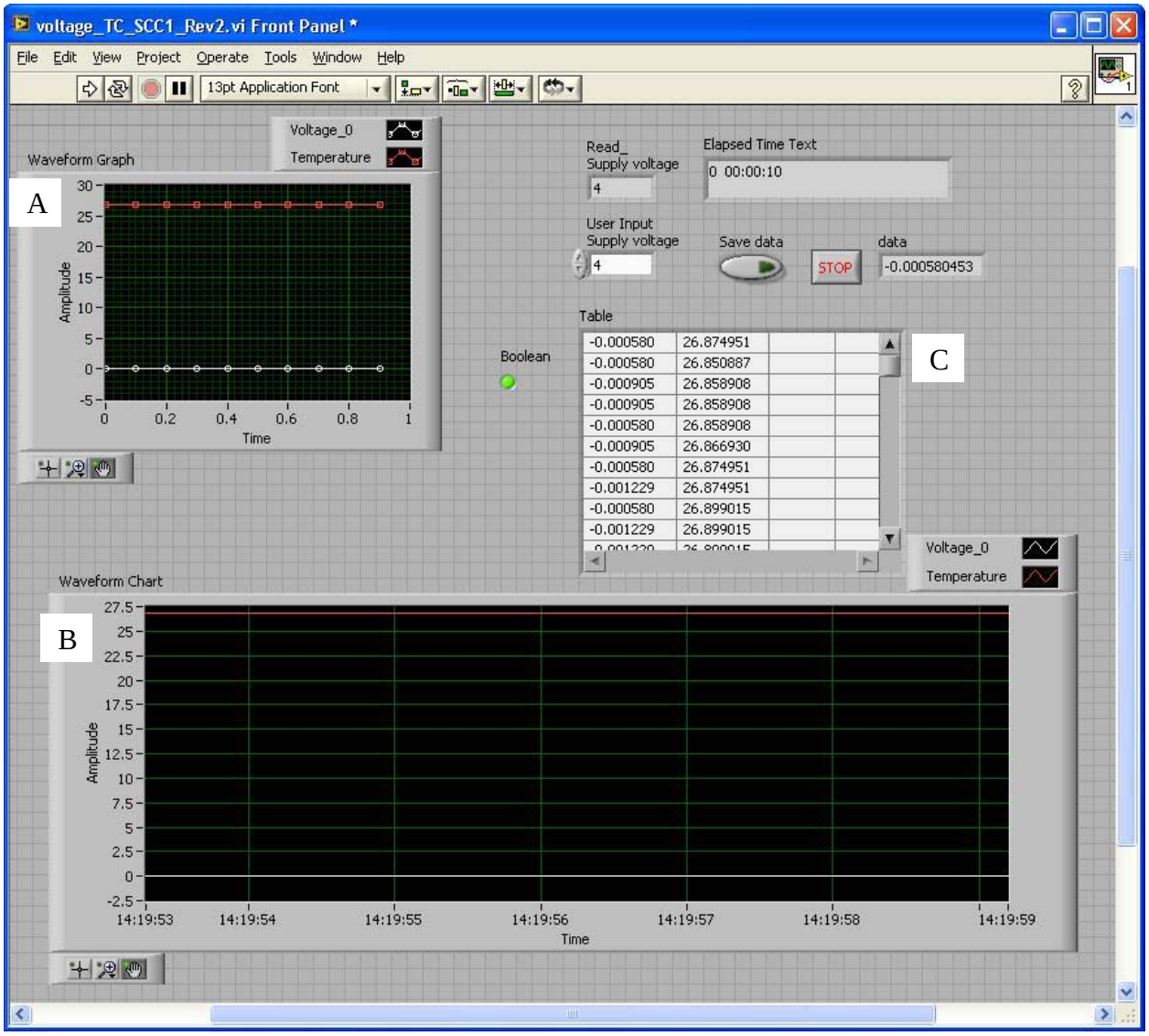

Figure 3-4. Labview GUI for data acquisition during valve testing. A) Shows temperature and voltage data for 10 samples over a second. B) Real time temperature and voltage data acquired. C) Numerical values of data acquired. D) Block diagram of the Labview program

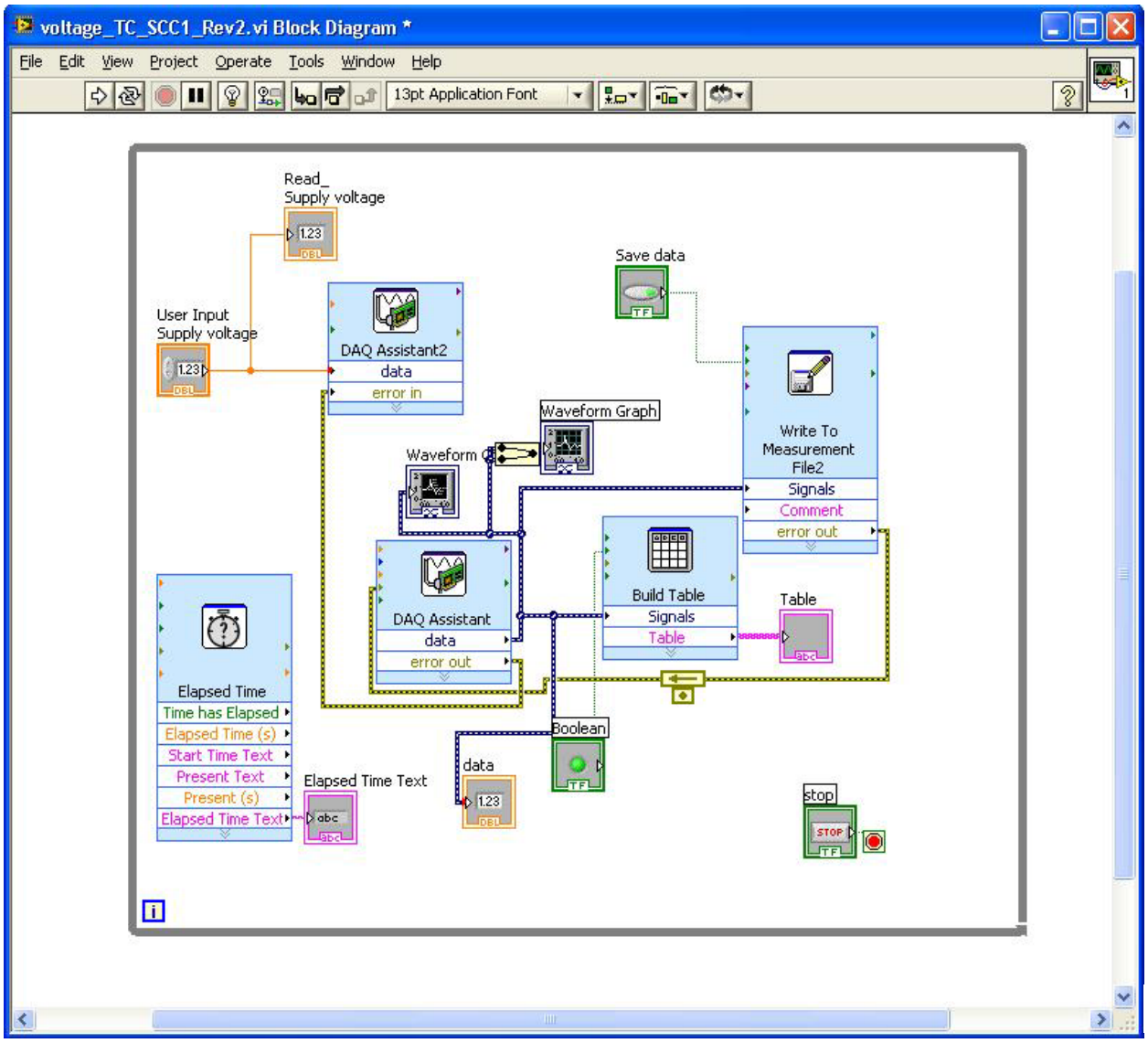

D

Figure 3-4. Continued

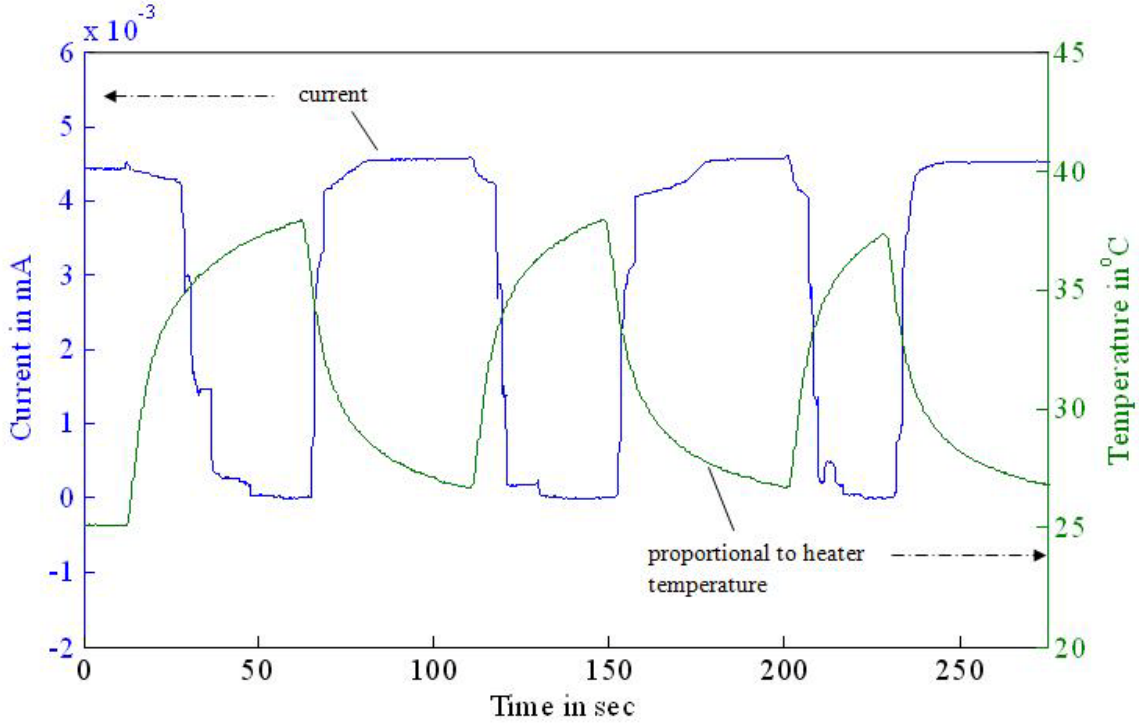

Figure 3-5. Valve actuation when 58 mW was applied to Au heaters. A hydrostatic head of 9.5 mm drives the flow. The channel conductivity and the temperature corresponding to resistive heater are shown in the plot as a function of time.

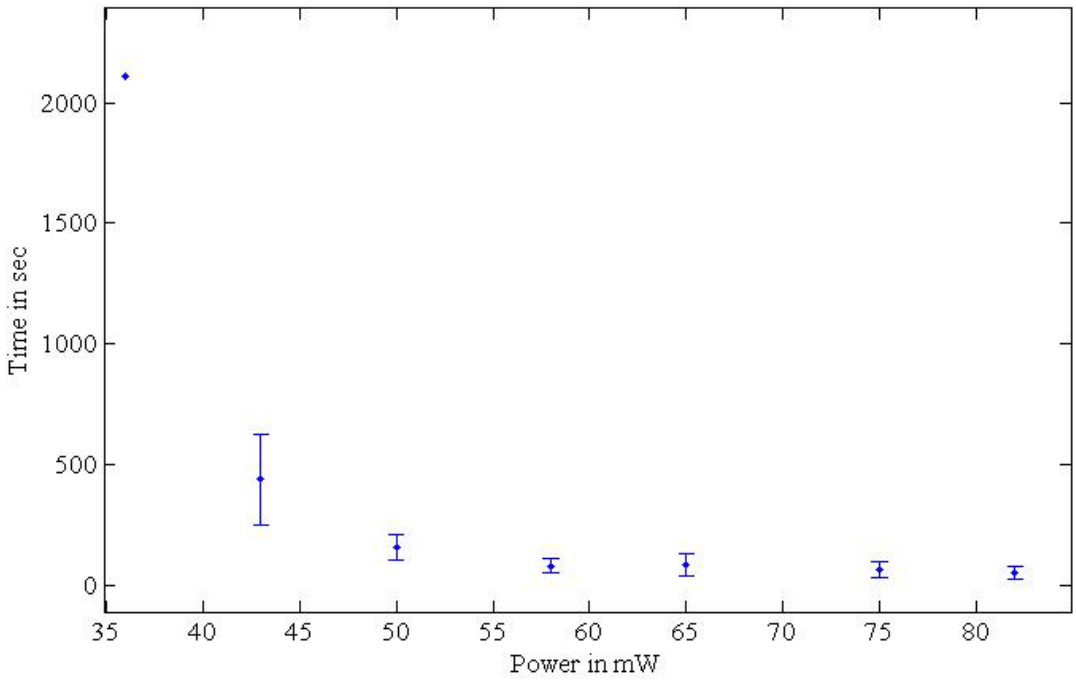

Figure 3-6. Valve actuation time as a function of the input power. Error bars indicate one standard deviation and a hydrostatic head of 9.5 mm drives the flow of 1M NaCl salt solution.

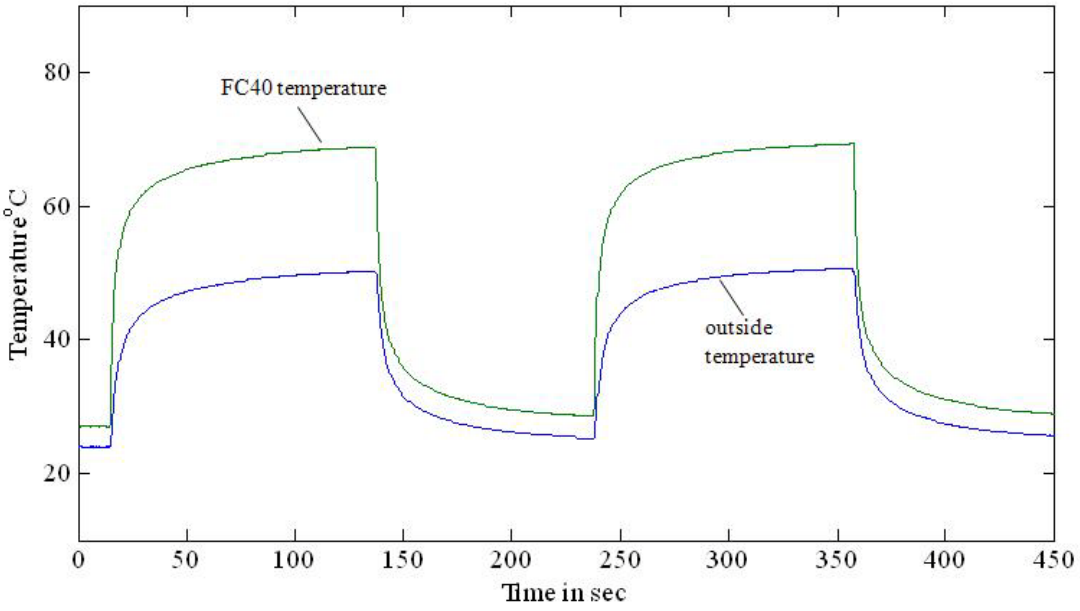

A

Figure 3-7. Temperature at different locations during valve actuation at 58 mW input heater power. A) Temperature of FC40 is measured using a K type thermocouple. The outside temperature is used as a comparative reference. B) Temperature measured in the microfluidic channel at a distance of 0.2 mm from well edge. C) Schematic showing thermocouple location in the device

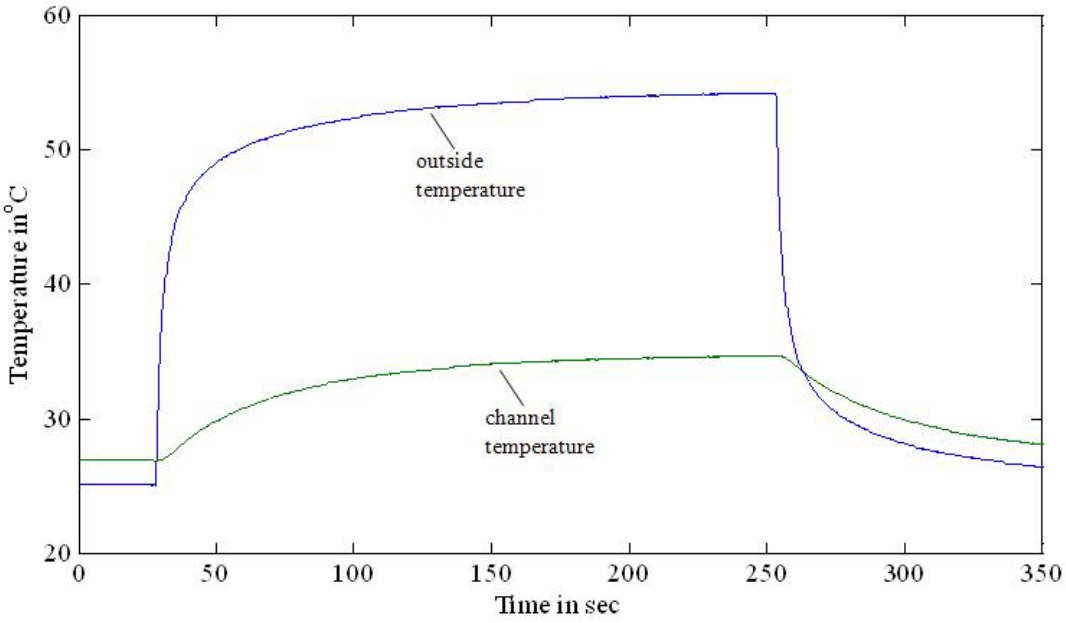

B

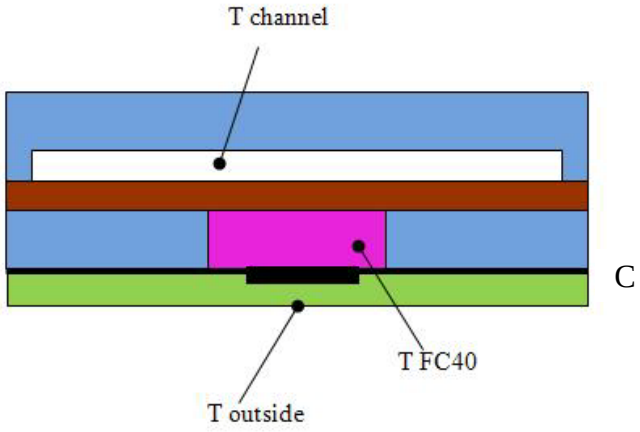

C

Figure 3-7. Continued.

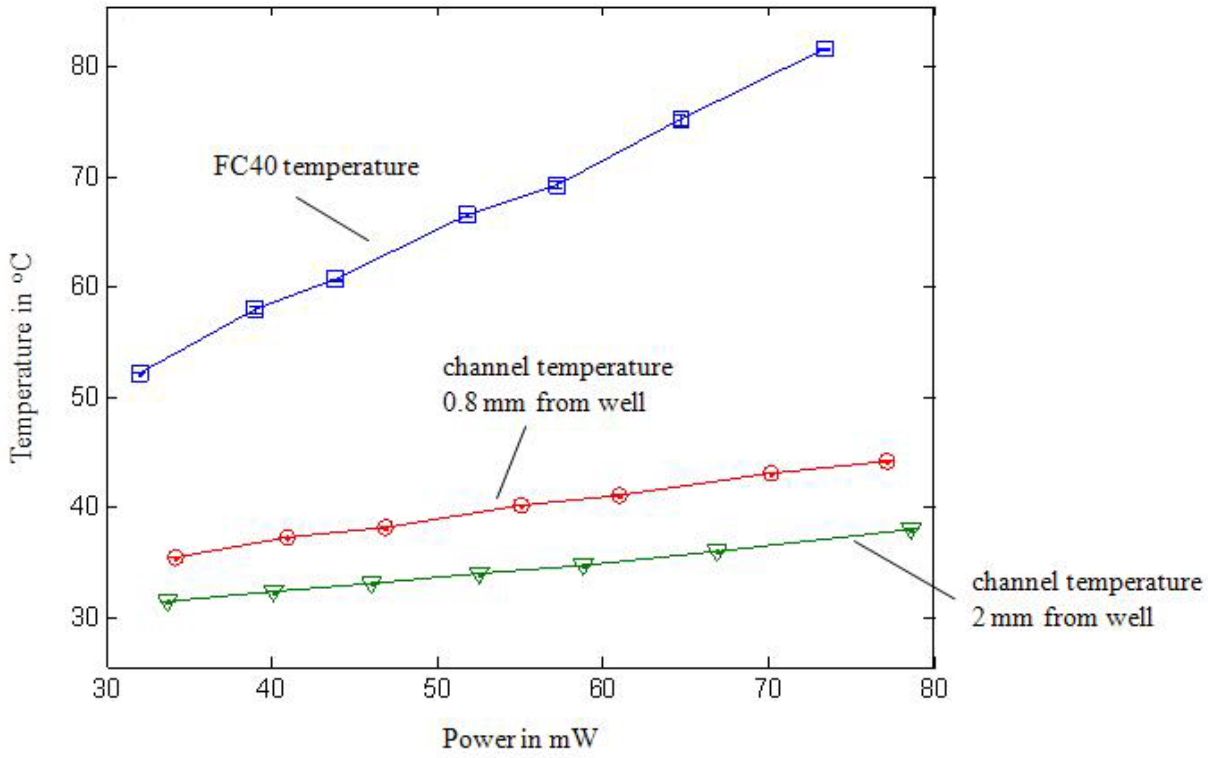

Figure 3-8. Temperature at different locations of a microvalve as a function of power.

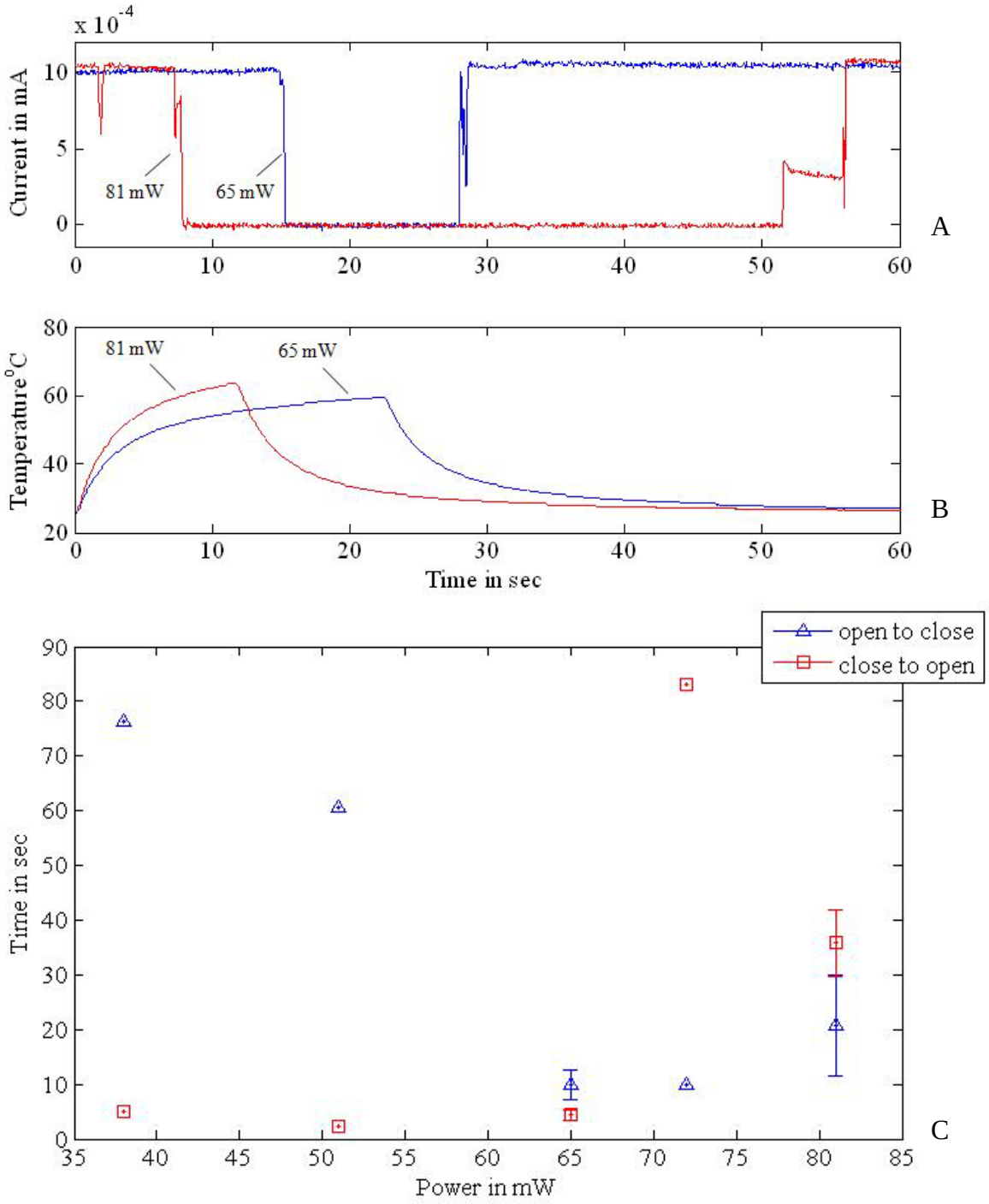

Figure 3-9. Valve actuation for a 300 nL/min flow with different heater input powers. A) Current through the microfluidic channel. B) Temperature on the exposed side of a heater film across the FC40 well. Higher powers result in higher temperature in shorter times and thus faster valve action, however, slower valve release to its initial off state. C) Valve time constants as a function of power.

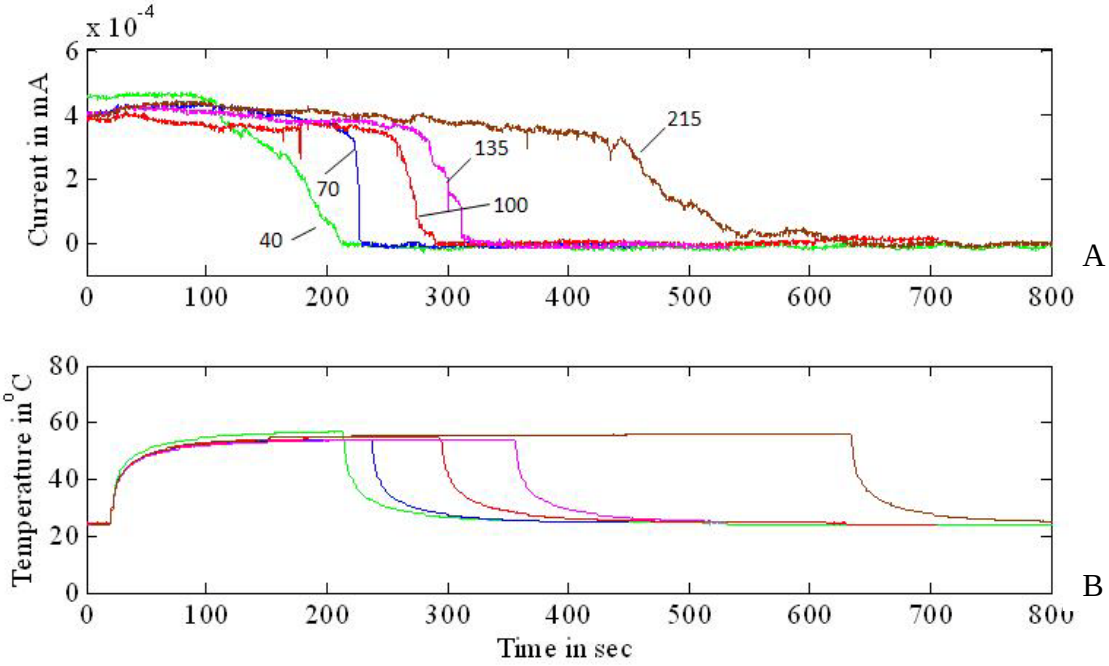

Figure 3-10. Electric current as a function of time when different hydrostatic heads were used. The pressure heads are in mm of 0.1M NaCl. The power was kept constant at 55 mW for all the tests. Rolling time averaging ,over 0.3 sec (every 3 consecutive data points), was used to smoothen the curve. A) Channel conductivity. B) Temperature corresponding to input power.

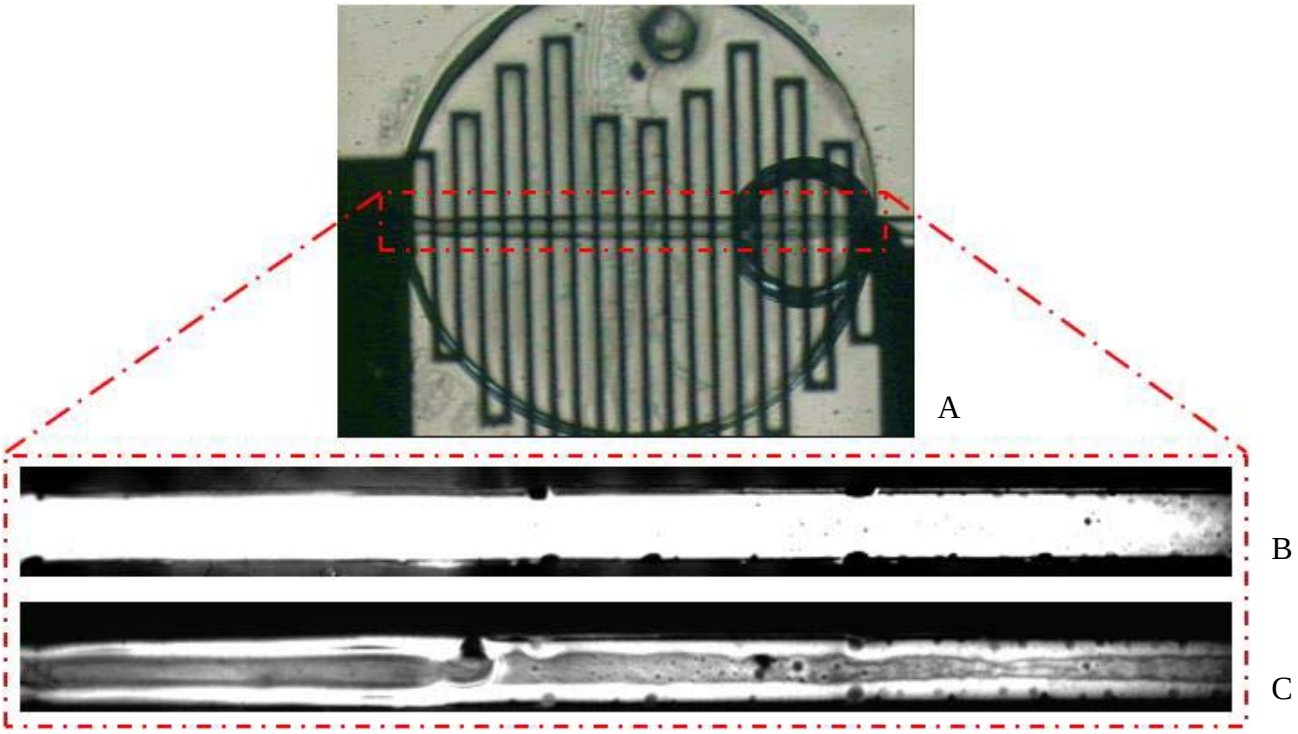

Figure 3-11. Fluorescent images showing valve action. Images are captured in the FC40 well showing the valve open to closed action. The reduction in fluorescence intensity shows the elastomer deflection in the valve area of microfluidic channel resulting in displacement of fluorescent dye. A) Filled FC40 well over the microfluidic channel. B) Valve open state with fluorescent dye filled in channel. C) Valve closed state wherein the PET film deflects into channel and displaces the dye.

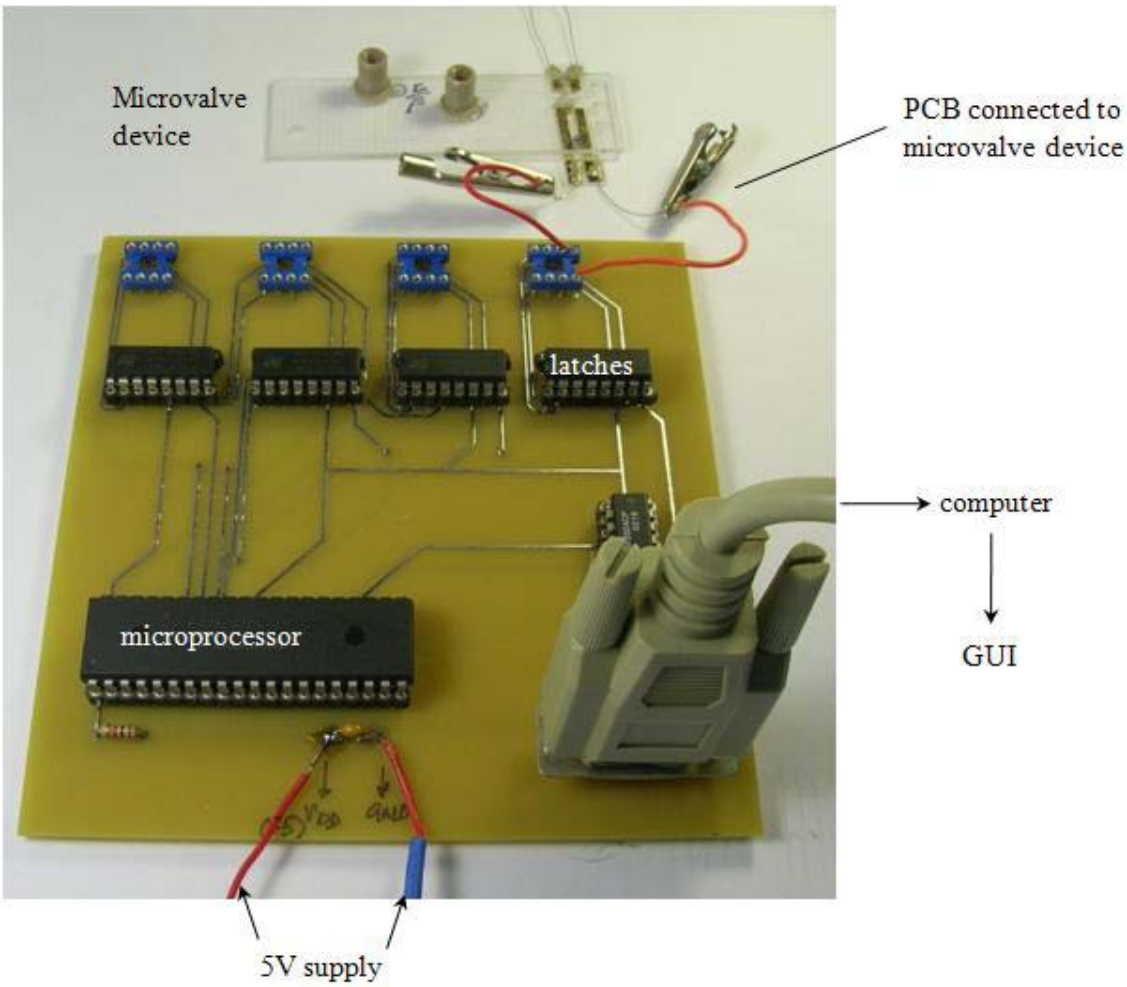

Figure 3-12. The PCB connected to a microvalve device

CHAPTER 4
CONCLUSIONS AND FUTURE WORK

A thermally actuated microfluidic valve has been fabricated and its operation has been demonstrated. The principle of the valve is based on thermal expansion of a fluid that deflects an elastomeric film into a microfluidic channel. Heat is supplied by a lithographically patterned heater. The power input to the microvalve can be controlled by a PCB.

4.1 Microvalve Fabrication

The microvalve has been fabricated with an aim to extend the concept to large scale integration. The valve is made of polymers and the bulk of the material used was cyclo olefin polymer with the elastomeric film being polyester. All plastic assembly helps to achieve lower device cost and faster fabrication times. The channel layer was injection molded and the remaining layers are assembled onto that layer by lamination, making it suitable for industrial mass production.

4.2 Microvalve Operation

4.2.1 Evaluation Using a Flow Meter

The microvalve was tested using two methods one is to use a micro-flowmeter while the other is electrical current measurement. The conclusions using each is summarized below.The first method used a commercial micro flow meter. The flow meter was connected downstream to measure the flowrate during valve action. Prior to valve testing, the flowmeter was evaluated for accuracy based on weight measurement. Tests were also performed to determine the effect of stiff and flexible connecting tubing, as well as the effects of the microfluidic channel. In addition, the pulsations produced by the syringe pump were studied. The results show that stiff tubing should be used for applications that require accurate flow control. The microflow meter was required for flow evaluation. When connected downstream the flowmeter showed the valve

actuation dynamics. The flow meter showed the flow rate go to zero when the valve was closed and back to the original value when it was open. During the operation, the pumping action due to membrane deflection was also observed, indicated by a hump or increase in flow rate. The flowmeter also showed that a longer valve close time with constant syringe pump supply resulted in higher pressure built up at the valve entrance. This was indicated by an increase in flow rate beyond the syringe pump rate once the valve is opened. The valve was tested reliably for a 300 nL/min (1.2 mm/s) flow supplied by a syringe pump.

Although the flowmeter gives the flow rate variation during valve action it had certain limitations. The flowmeter could not be connected near the valve region; as a result, the actual local flow changes could not be monitored. Connecting the flow meter downstream showed flow variations, which were due to flow reversals downstream and the pumping action. Hence a new method was developed to measure local valve actuation.

4.2.2 Electric Current Measurement

The channel conductivity was measured to study the local effect of valve actions. This method also demonstrated repetitive valve operation. It was found that the valve open-and-close cycles were in coherence with the heater input, which was proportional to the temperature in the valve. The valve could be operated over a wide range of power from 36 mW to 80 mW. The power controls the actuation times, typically a few seconds. The temperature in a channel during operation was found to be less than 45^{o}C, which is within the maximum temperature allowed before enzymes denature.[72] The valve was reliably tested at a flowrate of 300 nL/min (1.2 mm/s). Valve actuation was also demonstrated for an inlet pressure of 2000 Pa corresponding to 215 mm hydrostatic head. A valve can operate as many as 50 times.

Electric current measurement was advantageous since instantaneous change in the cross section due to elastomer deflection could be monitored. The downstream effects seen in the flow

meter method were overcome. However, any leakage currents through conductive parts could result in an erroneous measurement. Interfacial layer of thin conductive fluid could also result in errors.

The valve operation was also validated by fluorescence measurement in the actual valve region. Fluorescent solution filled in the channel was displaced due to valve action. The valve was also shown to be operable when it is connected with a PCB.

4.3 Future Work

Our study demonstrated the concept of a thermally actuated valve. Since the elastomer film used in the device has uniform adhesive coat on all areas, channel region is partially exposed to the membrane glue. The presence of glue results in hysteresis due to sticking effect. Hence, the adhesive should be removed locally in the future to improve the valve suitability to biological applications. The presence of glue can contaminate samples. With respect to channel geometry, the aspect ratio of the channel can be made less stringent for e.g. 10:1[19] rather than presently used 2.4:1.The single device fabrication process should be extended to an array of valves and all of them should be controlled using a PCB. The valve testing can also be improved if a pressure sensor is used in conjunction with a flowmeter. A pressure sensor connected upstream will enable monitor the pressure rise in the valve inlet during operation. It will also help define the maximum operation pressure[66] that the valve can withstand without delamination. In addition, a flow meter that can be integrated in the microchannel will enable local flow rate measurement.

LIST OF REFERENCES

1. R. P. Feynman, *Microelectromechanical Systems, Journal of*, 1992, **1**, 60-66.

2. J. S. Kilby, *Proceedings of the IEEE*, 2000, **88**, 109-111.

3. S. C. Terry, J. H. Jerman and J. B. Angell, *IEEE Trans. Electron Devices*, 1979, **26**, 1880-1886.

4. K. E. Petersen, *Proceedings of the IEEE*, 1982, **70**, 420-457.

5. A. Manz, N. Graber and H. M. Widmer, *Sens. Actuator B-Chem.*, 1990, **1**, 244-248.

6. G. M. Whitesides, *Nature*, 2006, **442**, 368-373.

7. W. M. Kurt Petersen, Gregory Kovacs, Allen Northrup, Lee Christel, and Farzad Pourahmadi, in *IVD Technol. Mag.*, 1998, pp. 43-49.

8. D. J. Harrison, K. Fluri, K. Seiler, Z. H. Fan, C. S. Effenhauser and A. Manz, *Science*, 1993, **261**, 895-897.

9. M. A. Burns, B. N. Johnson, S. N. Brahmasandra, K. Handique, J. R. Webster, M. Krishnan, T. S. Sammarco, P. M. Man, D. Jones, D. Heldsinger, C. H. Mastrangelo and D. T. Burke, *Science*, 1998, **282**, 484-487.

10. A. M. Skelley, J. R. Scherer, A. D. Aubrey, W. H. Grover, R. H. C. Ivester, P. Ehrenfreund, F. J. Grunthaner, J. L. Bada and R. A. Mathies, *Proc. Natl. Acad. Sci. U. S. A.*, 2005, **102**, 1041-1046.

11. J. S. Marcus, W. F. Anderson and S. R. Quake, *Anal. Chem.*, 2006, **78**, 956-958.

12. T. Thorsen, S. J. Maerkl and S. R. Quake, *Science*, 2002, **298**, 580-584.

13. J. West, M. Becker, S. Tombrink and A. Manz, *Anal. Chem.*, 2008, **80**, 4403-4419.

14. S. Haeberle and R. Zengerle, *Lab Chip*, 2007, **7**, 1094-1110.

15. D. B. Weibel and G. M. Whitesides, *Curr. Opin. Chem. Biol.*, 2006, **10**, 584-591.

16. H. Becker and C. Gartner, *Anal. Bioanal. Chem.*, 2008, **390**, 89-111.

17. A. de Mello, *Lab Chip*, 2002, **2**, 31N-36N.

18. J. C. McDonald and G. M. Whitesides, *Accounts Chem. Res.*, 2002, **35**, 491-499.

19. M. A. Unger, H.-P. Chou, T. Thorsen, A. Scherer and S. R. Quake, *Science*, 2000, **288**, 113-116.

20. J. M. K. Ng, I. Gitlin, A. D. Stroock and G. M. Whitesides, *Electrophoresis*, 2002, **23**, 3461-3473.

21. H. K. Wu, T. W. Odom, D. T. Chiu and G. M. Whitesides, *Journal of the American Chemical Society*, 2003, **125**, 554-559.

22. S. R. Quake and A. Scherer, *Science*, 2000, **290**, 1536-1540.

23. S. K. Sia and G. M. Whitesides, *Electrophoresis*, 2003, **24**, 3563-3576.

24. Y. Liu, D. Ganser, A. Schneider, R. Liu, P. Grodzinski and N. Kroutchinina, *Anal. Chem.*, 2001, **73**, 4196-4201.

25. M. Hupert, W. Guy, S. Llopis, H. Shadpour, S. Rani, D. Nikitopoulos and S. Soper, *Microfluid. Nanofluid.*, 2007, **3**, 1-11.

26. Q. Mei, Z. Xia, F. Xu, S. A. Soper and Z. H. Fan, *Anal. Chem.*, 2008, **80**, 6045-6050.

27. C. K. Fredrickson, Z. Xia, C. Das, R. Ferguson, F. T. Tavares and Z. H. Fan, *J. Microelectromech. Syst.*, 2006, **15**, 1060-1068.

28. K. W. Oh and C. H. Ahn, *J. Micromech. Microeng.*, 2006, **16**, R13-R39.

29. B. Bae, J. Han, R. I. Masel and M. A. Shannon, *J. Microelectromech. Syst.*, 2007, **16**, 1461-1471.

30. I. Fazal and M. C. Elwenspoek, *J. Micromech. Microeng.*, 2007, **17**, 2366-2379.

31. H. Q. Li, D. C. Roberts, J. L. Steyn, K. T. Turner, O. Yaglioglu, N. W. Hagood, S. M. Spearing and M. A. Schmidt, *Sensors and Actuators A: Physical.Micromechanics section of Sensors and Actuators, based on contributions revised from the Technical Digest of the 16th IEEE International conference on Micro Electro mechanical Systems (MEMS 2003)*, 2004, **111**, 51-56.

32. W. H. Grover, A. M. Skelley, C. N. Liu, E. T. Lagally and R. A. Mathies, *Sensors and Actuators B: Chemical*, 2003, **89**, 315-323.

33. M. L. A. H. Zdeblick, CA), The Board of Trustees of the Leland Stanford Junior University (Stanford, CA), United States, 1989.

34. A. K. Henning, J. Fitch, D. Hopkins, L. Lilly, R. Faeth, E. Falsken and M. Zdeblick, in *1997 International Conference on Solid State Sensors and Actuators, 1997. TRANSDUCERS '97 Chicago.*, 1997, pp. 825-828 vol.822.

35. X. Yang, C. Grosjean, Y.-C. Tai and C.-M. Ho, *Sensors and Actuators A: Physical.Tenth IEEE International Workshop on Micro Electro Mechanical Systems*, 1998, **64**, 101-108.

36. X. Yang, C. Grosjean and Y.-C. Tai, *Microelectromechanical Systems, Journal of*, 1999, **8**, 393-402.

37. C. A. Rich and K. D. Wise, *Microelectromechanical Systems, Journal of*, 2003, **12**, 201-208.

38. J.-H. Kim, K.-H. Na, C. J. Kang, D. Jeon and Y.-S. Kim, *Microelectronic Engineering.Micro and Nano Engineering 2003*, 2004, **73-74**, 864-869.

39. H. Takao, K. Miyamura, H. Ebi, M. Ashiki, K. Sawada and M. Ishida, *Sensors and Actuators A: Physical*, 2005, **119**, 468-475.

40. S. Vyawahare, S. Sitaula, S. Martin, D. Adalian and A. Scherer, *Lab Chip*, 2008, **8**, 1530-1535.

41. D. J. Beebe, J. S. Moore, J. M. Bauer, Q. Yu, R. H. Liu, C. Devadoss and B.-H. Jo, *Nature*, 2000, **404**, 588-590.

42. D. T. Eddington and D. J. Beebe, *Microelectromechanical Systems, Journal of*, 2004, **13**, 586-593.

43. E. T. Carlen and C. H. Mastrangelo, *Microelectromechanical Systems, Journal of*, 2002, **11**, 408-420.

44. R. H. Liu, J. Bonanno, J. Yang, R. Lenigk and P. Grodzinski, *Sensors and Actuators B: Chemical*, 2004, **98**, 328-336.

45. G. V. Kaigala, V. N. Hoang and C. J. Backhouse, *Lab Chip*, 2008, **8**, 1071-1078.

46. C. H. Ahn, J.-W. Choi, G. Beaucage, J. H. Nevin, J.-B. Lee, A. Puntambekar and J. Y. Lee, *Proceedings of the IEEE*, 2004, **92**, 154-173.

47. M. Yamada and M. Seki, *Anal. Chem.*, 2004, **76**, 895-899.

48. S.Shoji., in *Microsystem technology in chemistry and life sciences*, ed. H. E. B. Andreas Manz, Holger Becker, Springer, 1999, p. 252.

49. G. T. Kovacs, *Micromachined Transducers SourceBook*, McGraw-Hill Higher Education, 1998.

50. L. A. Legendre, J. M. Bienvenue, M. G. Roper, J. P. Ferrance and J. P. Landers, *Anal Chem*, 2006, **78**, 1444-1451.

51. R. W. Fox and A. T. McDonald, *Introduction to fluid mechanics*, J. Wiley, New York, 1998.

52. C. K. Fredrickson and Z. H. Fan, *Lab Chip*, 2004, **4**, 526-533.

53. N. T. Nguyen, A. H. Meng, J. Black and R. M. White, *Sensors and Actuators a-Physical*, 2000, **79**, 115-121.

54. N. T. Nguyen, *Flow Measurement and Instrumentation*, 1997, **8**, 7-16.

55. M. Ashauer, H. Glosch, F. Hedrich, N. Hey, H. Sandmaier and W. Lang, *Sensors and Actuators a-Physical*, 1999, **73**, 7-13.

56. E. Kjeang, B. Roesch, J. McKechnie, D. A. Harrington, N. Djilali and D. Sinton, *Microfluidics and Nanofluidics*, 2007, **3**, 403-416.

57. X. H. Huang, M. J. Gordon and R. N. Zare, *Analytical Chemistry*, 1988, **60**, 1837-1838.

58. D. K. Kim, A. Majumdar and S. J. Kim, *Sensors and Actuators a-Physical*, 2007, **136**, 80-89.

59. J. G. Santiago, S. T. Wereley, C. D. Meinhart, D. J. Beebe and R. J. Adrian, *Experiments in Fluids*, 1998, **25**, 316-319.

60. C. Helmbrecht, R. Niessner and C. Haisch, *Analytical Chemistry*, 2007, **79**, 7097-7103.

61. G. R. Wang, I. Sas, H. Jiang, W. P. Janzen and C. N. Hodge, *Electrophoresis*, 2008, **29**, 1253-1263.

62. U. Kanne and C. Sauvain, *Medical Device Technology*, 2006, **June**.

63. U. Kanne, T. Preiswerk and G. Bohm, *Lc Gc Europe*, 2003, **16**, 65-66.

64. S. Kar, S. McWhorter, S. M. Ford and S. A. Soper, *Analyst*, 1998, **123**, 1435-1441.

65. J. M. Kohler and P. A. Gross, *Microfluidics and Nanofluidics*, 2007, **3**, 653-663.

66. G. F. Chen, F. Svec and D. R. Knapp, *Lab Chip*, 2008, **8**, 1198-1204.

67. W. H. Grover, M. G. von Muhlen and S. R. Manalis, *Lab Chip*, 2008, **8**, 913-918.

68. C. Das, C. K. Fredrickson, Z. Xia and Z. H. Fan, *Sens. Actuator A-Phys.*, 2007, **134**, 271-277.

69. D. B. Weibel, M. Kruithof, S. Potenta, S. K. Sia, A. Lee and G. M. Whitesides, *Anal. Chem.*, 2005, **77**, 4726-4733.

70. T. I. Wallow, A. M. Morales, B. A. Simmons, M. C. Hunter, K. L. Krafcik, L. A. Domeier, S. M. Sickafoose, K. D. Patel and A. Gardea, *Lab Chip*, 2007, **7**, 1825-1831.

71. X. Huang, M. J. Gordon and R. N. Zare, *Anal. Chem.*, 1988, **60**, 1837-1838.

72. D. L. Purich, *Contemporary enzyme kinetics and mechanism*, Academic Press, San Diego, 1996.

73. J. M. C. Yungas A.Çengel, *Fluid mechanics : fundamentals and applications*, McGraw-HillHigher Education, Boston, 2006.

74. M. A. Unger, H. P. Chou, T. Thorsen, A. Scherer and S. R. Quake, *Science*, 2000, **288**, 113-116.

75. J. N. Lee, C. Park and G. M. Whitesides, *Anal. Chem.*, 2003, **75**, 6544-6554.

BIOGRAPHICAL SKETCH

Karthik was born and brought up in Nagpur, India. He earned his Bachelor of Engineering degree in mechanical engineering in June 2004 from National Institute of Technology Karnataka Surathkal. In August 2006, he enrolled at the University of Florida to pursue a Master of Science degree in mechanical engineering.